Development of Air-breathing Polymer Electrolyte Membrane (PEM) Fuel Cell for small UAV application

A thesis submitted to the
Graduate School of Natural and Applied Sciences

by

Noor Ul Hassan

in partial fulfillment for the
degree of Master of Science

in

Industrial and Systems Engineering

This is to certify that we have read this thesis and that in our opinion it is fully adequate, in scope and quality, as a thesis for the degree of Master of Science in Industrial and Systems Engineering.

APPROVED BY:

Assoc. Prof. Dr. Bahadır Tunaboylu (Thesis Advisor) .....

Asst. Prof. Dr. Murat Küçükvar .....

Asst. Prof. Dr. Furkan Dündar .....

This is to confirm that this thesis complies with all the standards set by the Graduate School of Natural and Applied Sciences of İstanbul Şehir University:

DATE OF APPROVAL: 13 August 2015

SEAL/SIGNATURE:

Declaration of Authorship

I, Noor Ul Hassan, declare that this thesis titled, 'Development of Air-breathing Polymer Electrolyte Membrane (PEM) Fuel Cell for small UAV application' and the work presented in it are my own. I confirm that:

- This work was done wholly or mainly while in candidature for a research degree at this University.
- Where any part of this thesis has previously been submitted for a degree or any other qualification at this University or any other institution, this has been clearly stated.
- Where I have consulted the published work of others, this is always clearly attributed.
- Where I have quoted from the work of others, the source is always given. With the exception of such quotations, this thesis is entirely my own work.
- I have acknowledged all main sources of help.
- Where the thesis is based on work done by myself jointly with others, I have made clear exactly what was done by others and what I have contributed myself.

Signed: 

Date: 13 August 2015

"The glory of man, made of clay; lies, in his ever fresh activities! The moon and the stars do what they have always been doing."

Allama Muhammad Iqbal

Development of Air-breathing Polymer Electrolyte Membrane (PEM) Fuel Cell for small UAV application

Noor Ul Hassan

Abstract

Polymer exchange membrane fuel cells (PEMFC) are the devices that directly convert Chemical energy into Electrical energy and are potential candidates for portable and stationary power supply applications due to their several advantages over combustion engines. This study has been carried out to develop Air breathing and air cooling PEM Fuel cell stack for small Unmanned Aerial Vehicle (UAV) application with a power requirement of 200 W. Keeping in view the available space and weight constraints of UAV, I have optimally designed the shape of active area (10 cm x 2 cm) and flow channels. Fluid flow analysis using ANSYS Fluent software was performed on different channel shapes and an optimal design (double serpentine), with least pressure drop and optimal velocity profiles, was selected. Electro-chemical simulations were also done to predict the fuel cell performance (IV and Power curves) using MATLAB software prior manufacturing the prototype. Moreover, for the sake of DOE targets, initial tests were performed on single cell. Bipolar plates were more focused in terms of alternate material, novel design and fabrication process. An alternate fabrication technique was studied to manufacture Expanded Graphite (EG) polymer composite bipolar plates. Cutting molds were designed to cut channels on thin (0.6 mm) commercially acquired EG sheets. Three separate sheets, with flow channel textures removed, were glued to each other by a commercial conductive epoxy to build a single bipolar plate. The final product was characterized in terms of electro-mechanical properties as well as density, weight and cost. Fabrication process devised can be good alternate for small scale as well as mass production. Moreover, a PEM fuel cell stack is provided with an appropriate clamping torque to prevent leakage of reactant gases and to minimize the contact resistance between gas diffusion media (GDL) and bipolar plates. GDL porous structure and gas permeability is directly affected by the compaction pressure which consequently drastically change the fuel cell performance. Single cell performance tests were performed at five different clamping torque values for achieving optimal cell performance. Experimental and theoretical results were compared for making inferences about optimal cell performance.

Keywords: PEM Fuel Cell, Simulations, Bipolar Plate, Graphite polymer composite, manufacturing technique, Clamping torque, Optimal cell performance

Küçük İHA Uygulamaları İçin Hava Dolaşımlı Polimer Elektrolit Zarlı Yakıt Hücre Geliştirilmesi

Noor Ul Hassan

Öz

Polimer zar değişim yakıt hücreleri kimyasal enerjiyi doğrudan elektrik enerjisine çevirebilen cihazlar (donanım-aygıt) olmakla birlikte içten yanmalı motorlara olan bazı üstün özellikleri sayesinde taşınabilir veya sabit güç kaynağı uygulamalarına potansiyel bir alternatif olarak sunulabilir. Bu çalışma, güç gereksinimi 200W ın altında olan küçük insansız hava araçları uygulamaları için hava dolaşımlı (solumalı) ve hava soğutmalı PEM yakıt hücreleri geliştirmek için yürütülmüştür. İnsansız Hava Araçları(İHA) hacim ve ağırlık kısıtlamalarını göz önünde tutarak, aktif alan formunu (10 x 2 cm^2) ve akış kanallarını en optimum şekilde tasarladm. Akışkanlar Mekaniği analizi, ANSYS Fluent yazılım programı kullanılarak, en az basınç düşümü ve optimum hız profilleri seçilerek, farklı kanal şekilleri ve optimum dizayn (çift dönüşlü) için gerçekleştirilmiştir. Prototip üretimi öncesinde MATLAB programı ile Elektrokimyasal simülasyonlar yakıt hücresi performansını (IV ve Güç Eğrileri) üngürebilmek için yapılmıştır. Ayrıca, DOE hedefleri için, ilk testler tek bir hücre üzerinde yapılmıştır. Çift kutuplu levhalara sırasıyla malzeme, özgün tasarım ve üretim prosesi açısından odaklanılmıştır. Expanded Graphite (EG) polimer kompozit çift kutuplu levhaların imalatı için alternatif bir öretim tekniği üzerinde çalışılmıştır. Kesme kalıpları, kanalları ticari olarak belirlenmiş 0.6 mm kalınlığında EG tabakaları kesebilmek için dizayn edilmiştir. Bir tek çift polar levha oluşturabilmek için akış kanalları kaldrılmış üç ayrı tabaka, ticari iletken epoxy ile birbirine yapıştırılmıştır. Nihai ürün, elektro mekanik özellikleri yönünden olduğu gibi yoğunluk, ağırlık ve maliyet ile de karakterize edilebilir. Planlanmış üretim prosesi, hem küçük ölçekli üretim için hem de seri üretim için güzel bir alternatif olabilir. Yukarıdaki çalışmalara ek olarak, reaktif gazların sızıntısını engellemek ve gaz yayım aracı (gas diffusion media, GDL) ve çift kutuplu levhalar arası kontak direncini azaltmak amacıyla PEM yakıt hücresi uygun bir sıkma torku ile sıkıştırılır. Gözenekli yapısı ve gaz geçirgenliği ile GDL, yakıt hücresinin performansını önemli ölçüde değiştiren sıkıştırma basıncından doğrudan etkilenir. Optimum hücre performansını elde etmek amacıyla, tek hücre performans testleri beş farklı sıkma torku değerlerinde gerçekleştirilmiştir. Optimum hücre performansı hakkında sonuçlar çıkarabilmek için deneysel ve teorik sonuçlar karşılaştırılmıştır.

Anahtar Sözcükler: PEM Yakit hücresi, Simülasyonlar, çift kutuplu plaka, Grafit polimer kompozit, üretim teknikleri, Sikma torku, Optimum Hücre performans

Dedicated to my sister, "Noor Fatima",who cared for me like mother and shared my secrets like the best friend.

Acknowledgments

I would like to express my utmost gratitude to Dr. Bahadır Tunaboylu for his supervision guidance and feedback. The project has been a collaborate effort between Gebze Technical University (GTU) and TÜBITAK (Hydrogen and Fuel cell Laboratory). GTÜ funded a research project for developing Polymer Electrolyte Membrane Fuel Cell (PEMFC) for small Unmanned Aerial Vehicle (UAV). Prof. Dr. Ali Ata and Dr. Furkan Dündar have been providing me necessary material and equipment support for successful accomplishment of this project at GTÜ. Special thanks to Dr. Suha Yazıcıand Dr. Emin Okumuş for their valuable guidance and help while doing my experiments at TÜBITAK. I would like to thank them for all their help and guidance I have received. Most of all, the prayers of my mother and my wife's support, without them I would have not been able to achieve success.

Contents

List of Figures

Abbreviations

PEFC	**P**olymer **E**lectrolyte **F**uel **C**ell
PEMFC	**P**olymer **E**lectrolyte **M**embrane **F**uel **C**ell
SOFC	**S**olid **O**xide **F**uel **C**ell
AFC	**A**lkaline **F**uel **C**ell
PAFC	**P**hosphoric **A**cid **F**uel **C**ell
MCFC	**M**olten **C**arbonate **F**uel **C**ell
UAV	**U**nmanned **A**erial **V**ehicle
FCV	**F**uel **C**cell **V**ehicle
DOE	**D**epartment **O**f **E**nergy
MEA	**M**embrane **E**lectrode **A**ssembly
BPP	**B**ipolar **P**late
GDL	**G**as **D**iffusion **L**ayer
ICE	**I**nternal **C**ombustion **E**ngine
EG	**E**xpanded **G**raphite
GHG	**G**reen **H**ouse **G**ases
PFSA	**P**er **F**luoro **S**ulfonic **A**cid
PTFE	**P**oly **T**etra **F**luoro **E**thylene
CNC	**C**omputer **N**umerical **C**ontrol
GFC	**G**as **F**low **C**hannel

Physical Constants

Ideal Gas constant	R	=	8.314 $J.mol^{-1}.K^{-1}$
Faraday's constant	F	=	96487 Coulombs

Symbols

Symbol	Name	Unit
U	Potential difference or Voltage	Volts(V)
I	Current	Ampere (A)
P	power	W (Js^{-1})
A	Area	cm^2)
J	Current Density	(Acm^{-2})
R	Resistance	Ohm (Ω)
U_{cell}	Fuel cell output Voltage	Volts(V)
E_{Nernst}	Reversible Voltage	Volts(V)
U_{act}	Activation potential drop	Volts(V)
U_{Ω}	Ohmic potential drop	Volts(V)
U_{con}	Concentration potential drop	Volts(V)
U_s	Stack Voltage	Volts(V)
T	Temperature	Kelvin(K)
P_{H2}	Effective partial pressure of Hydrogen	atm
P_{O2}	Effective partial pressure of Oxygen	atm
RH_a	Relative Humidity at Anode	Percent
RH_c	Relative Humidity at Cathode	Percent
P_{H2O}	Effective partial pressure of water	atm
ξ	Parametric Coefficient	no unit
CO_2	Concentration of dissolved Oxygen	(mol/cm_3)
R_M	Membrane resistance	Ohm (Ω)
λ	Water content of membrane	no unit
T_t	Tightining Torque	N.m
F_{clamp}	Clamping Force	N

D_b	Bolt Nominal Diameter	meters(m)
K_b	Friction Coefficient	no unit
N_b	Number of bolts	no unit
(P_c)	Clamping pressure	$N.m^{-2}$

Chapter 1

Introduction to Fuel Cells

1.1 Motivation

The anthropogenic contribution to global warming has been evident for some time. To reduce the impact we have on the climate, it is important to minimize the use of fossil fuels. A potential energy carrier that can replace fossil fuels is hydrogen. Hydrogen can be made from water splitting, and can be made sustainable with the use of renewable energy. This can afterwards be converted to electrical energy in a fuel cell, without any emissions other than water. Fuel cells can be a promising candidate for fulfilling our future energy demands. Fuel cells are generally categorized on the basis of electrolyte used. According to Papageorgopoulos et al. review, They can be defined as Electrochemical devices that directly convert chemical energy stored in fuels such as hydrogen to electrical energy. The efficiency of fuel cells can be obtained as much as sixty percent in terms of electrical energy conversion. Overall eighty percent in co-generation of electrical and thermal energies with greater than ninety percent reduction in major pollutants can be obtained [1]. Fuel cells can be grouped into five major types as itemized below. For the last couple of decades, these five categories of fuel cells have been extensively researched.

1. Proton / Polymer Electrolyte Membrane (PEM) Fuel Cells (sometimes abbreviated as PEFCs),
2. The Solid Oxide Fuel cells (SOFCs),

3. Alkaline Fuel Cells (AFCs),
4. Phosphoric-Acid Fuel cells (PAFCs),
5. Molten Carbonate Fuel Cells (MCFCs).

1.2 PEM Fuel Cells

Polymer electrolyte membrane (PEM) fuel cells are considered to be the most advantageous type of fuel cell. PEM fuel cells use a polymer electrolyte membranes (renowned with the name Nafion) as proton conducting media and Platinum (Pt) based materials as catalyst. Fuel cell technology is not very recent, The first fuel cell was invented by Sir William Robert Grove in 1839. Details can be found in reference [2]. PEM fuel cells traditionally use hydrogen as the fuel. PEM fuel cell work similar to a battery, it is generally composed of a cathode and an anode electrode, that are separated by a polymer electrolyte membrane. The fuel, hydrogen in this case, is fed continuously to the anode, and the Oxygen or air, is fed continuously to the cathode. Hydrogen gas molecules split into protons and electrons by the action of catalyst producing heat as a byproduct. Electrons travel via external circuit giving useful electrical energy while Protons move through the membrane. They meet with Oxygen at cathode and react together to produce water and heat. Many other types of fuels can also be fed to PEM fuel cells, like biomass derived materials and ethanol etc. These fuels need to be fed to a reformer first to extract pure Hydrogen and then inputted to PEM fuel cell. [3]. A mechanical model of single PEM fuel cell drawn in SolidWorks software is shown in Figure 1.1. The prominent features of PEM fuel cells can be itemized as follows;

1. Higher power density (W/cm^2)
2. Compactness (kW/L)
3. Light weight (kW/kg)
4. Operating Temperature range (50-80 ∘C)
5. Start-up / Stop time (0-2 min)
6. Quicker response to load variations (0-30 sec)

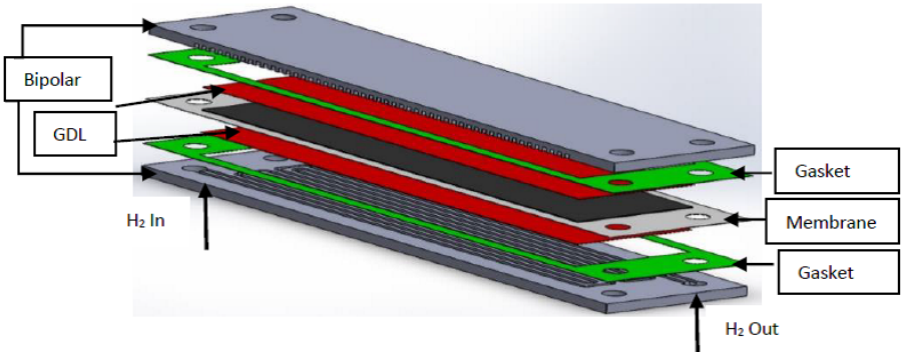

FIGURE 1.1: Mechanical model of single PEM fuel cell

The Hydrogen (H_2) and Oxygen (O_2) have a strong chemical affinity, and the chemical reactions of the PEM fuel cell are formulated as follows:

Oxidation reaction at the anode:

$2H_2 \longrightarrow 4H^+ + 4e^-$

Reduction reaction at the cathode:

$4H^+ + 4e^- + O_2 \longrightarrow 2H_2O$

Overall reaction:

$2H_2 + O_2 \longrightarrow 2H_2O$

During electro-chemical reactions and electron transfer process, an electromotive force is generated between the two electrodes. Many single cells can be assembled into a fuel cell stack in order to obtain the required amount of power. Importantly, the PEM fuel cell needs a quite low operating temperature, which typically ranges from 50 to $80°C$, and is very safe in applications [4]. Fuel cells, more specifically PEM type have several advantages over Internal Combustion (IC) engines. A few are illustrated in the Figure 1.2 below.

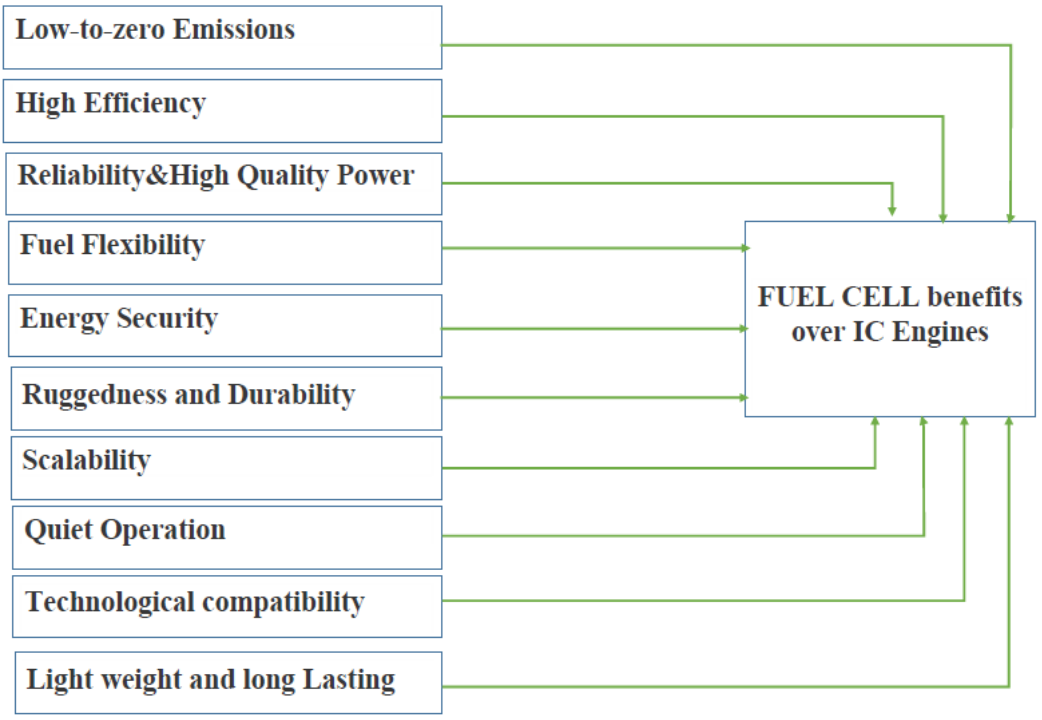

FIGURE 1.2: Fuel cell benefits over conventional Internal Combustion (IC) engine

1.2.1 PEM Fuel Cell Components

A typical PEM fuel cell consists of a cell stack, water and thermal management sub-systems, Hydrogen and Oxygen management sub-systems, and a power conditioning and control system module. A cell stack is an assembly of membranes, catalyst layers, gas diffusion layers (GDL), bipolar plates (BPP) and seals. The PEM fuel cell stack is a combination of several flow systems, i.e., electrical, chemical, fluid and heat flows. The stack is a serial combination of unit cells to generate the designed power output. With the increasing number of unit cells in a stack, PEM fuel cells show some losses of efficiency and power density. PEM fuel cell stack assembly process, component quality, mutual contact between the components, etc. may contribute to significant performance degradation. Following listed components are crucial and subject to improvement in terms of material, design, manufacturing process etc.

1. Bipolar plates with Gas flow channels (Anode and Cathode)
2. Gas diffusion Layer (GDL)
3. Membrane (coated with catalyst layer on both sides)

4. Seal / Gasket
5. Current Collectors / Electrodes
6. End Plates

A schematic diagram of PEM type fuel cell components labeled is shown in Figure 1.3.

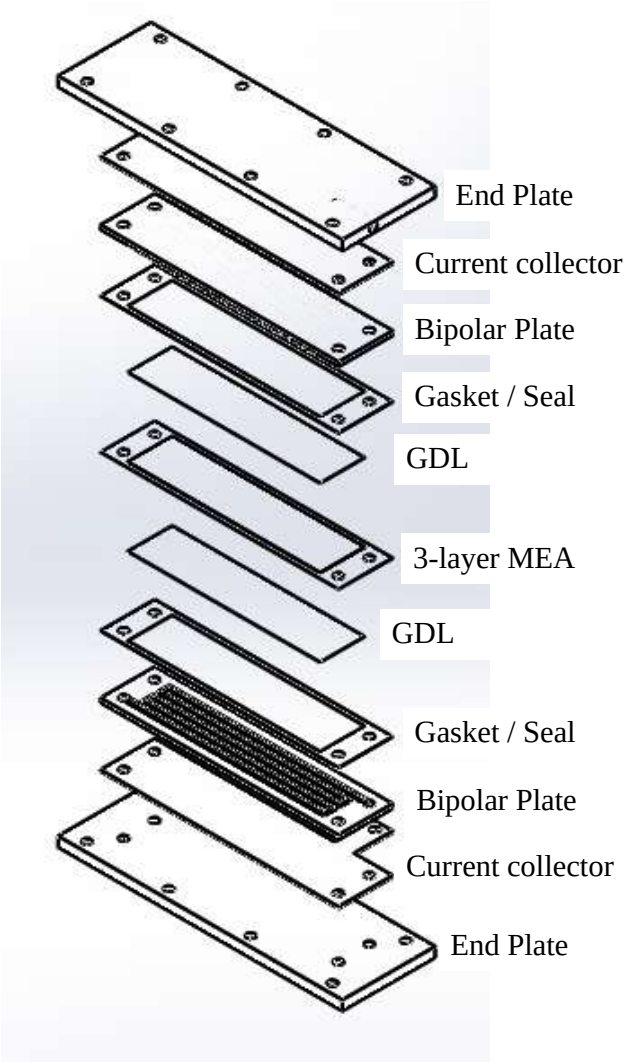

FIGURE 1.3: PEM fuel cell components

1.2.2 Technical Targets for PEM Fuel cells

US Department of Energy (DOE) has initiated a program to meet energy demands and search for alternate environmentally friendly power sources. For making PEM fuel cells commercially feasible, DOE has set some targets that range from technical specifications as well as physical and cost parameters. The main emphasis on technical targets is to develop efficient materials, components, and fuel cell subsystems which make fuel cells to achieve the Fuel Cells sub-program objectives. The key features are related to system cost and durability. Following are some of the parameter targets set by DOE for PEM fuel cells transportation applications for the year 2020 [5].

1. Energy efficiency (60 $ / kW)
2. Power density (850 W/L)
3. Cost (30 $ / kW)
4. Durability in automotive drive cycle (5000 hours)

1.2.3 Applications of PEM fuel cell technology

Pertaining to environment issues and greenhouse effects, transportation vehicles are considered to be the major contributors. To cater these important issues, PEM fuel cell finds its best application in transportation mainly because of their potential impact on the environment. Another main application include stationary and portable power production systems. Almost all renowned auto manufacturers have developed their fuel cell vehicles and they will soon launch their products in market. Main applications of PEM fuel cells can be summarized as below‘;

1. Vehicle transportation
2. Smaller scale stationary power generation
3. Auxiliary Power Units (APUs)
4. Portable powers for electronics

Besides attractive applications of PEM fuel cell, the high manufacturing cost and degradation / reliability issues remain the challenging barrier that prohibit their widespread applications in this area.

1.3 Research Objectives

The objective of this research is to develop comprehensive understanding of electrochemical models, simulations and manufacturing processes using different kinds of materials. Mathematical models and analysis tools were used to predict the performance of PEM fuel cells by incorporating assembly issues, contact resistance, component material properties, and operating conditions. These techniques can be utilized to improve fuel cell design and manufacturing to ensure robust performance. The specific tasks include:

1. The Development of Air-breathing PEM Fuel Cell for small UAV application using simulated results of bipolar flow field design and electro-chemical models.
2. Fabrication of bipolar plates with different material, novel design and manufacturing technique.
3. Experimental determination of optimal clamping torque for Air-breathing PEM fuel cell.

Fulfillment of the objectives will provide a comprehensive understanding of the fuel cell performance theoretically and then validation through experimentation. Then performance enhancement by changing the design,material and fabrication technique of one of the most important component (bipolar plate). The impact of assembly procedures and impact of assembly pressure on electrical contact resistance and performance in fuel cell stack assembly will be studied. In summary, results from this dissertation will lead to improved manufacturing and assembly of PEM fuel cells as well as improved performance.

1.4 Organization of dissertation

This dissertation is presented in a multiple manuscript format. Chapter 3, 4 and 5 are written as individual research articles, explaining the topic introduction, experimental procedures and results with discussion.

1. Chapter 1 provides the importance of the topic selected for study and its various aspects to be explored at an introductory level.

2. Chapter 2 covers the design of PEM fuel cell stack with necessary calculations. Further, it provides mechanical models with drawings generated using SolidWorks software. Finally, the whole process of prototype manufacturing process is explained at lab scale showing equipment used for manufacturing and testing.

3. Chapter 3 gives a problem based study to fabricate light weight, cost effective and reliable bipolar plates by utilizing the simulated results for achieving optimal experimental results. ANSYS Fluent software was used for analysis on different bipolar plate fuel flow channel designs. An optimal design with least pressure drop and optimal velocity profiles, was selected based on these simulation results. Electro-chemical simulations were also done to predict the fuel cell performance (IV and Power curves) using MATLAB software prior manufacturing the prototype.

4. Chapter 4 provides a comprehensive study of an alternate bipolar plate fabrication technique using different material and novel design. Expanded graphite composite material has been used for fabrication of bipolar plates. Emphasis has been done in fabrication process which has not been reported in literature before. Three separate sheets, with flow channel textures removed, were glued together by a commercial conductive epoxy to build a single bipolar plate. The final product obtained was characterized for its specific properties and performance.

5. Chapter 5 makes a detailed experimental demonstration of the effects of PEM fuel cell stack clamping torque on cell performance. Single cell performance tests were performed at various clamping torque values for achieving optimal cell performance. Experimental and theoretical results were compared for making inferences about optimal cell performance.

6. Chapter 6 draws the conclusions and summarizes the original contributions of the dissertation. Several topics are also proposed for future research.

Chapter 2

PEM Fuel Cell Design and Prototype Fabrication

2.1 Fuel Cell Stack Design / size calculations

The critical requirement for designing a PEM fuel cell systems is that it should be capable of delivering desired power output. For my system, a maximum power level of 200 W is required for Unmanned Aerial Vehicle (UAV) application operating at 24 V. Barbir et al. [6] explains a step by step design process for a specific application. Firstly, fuel cell active area and the number of cells to be joined in a stack must be determined. Application requirements provide the necessary requirements while designing a fuel cell stack for a specific application. These requirements may include desired power output, desired or preferred stack voltage or range of voltages, required efficiency, and volume and weight limitations. For fulfillment of a specific requirement, we may get a compromising solution for other requirements. So final design will be an optimized combination of desired parameters but providing the key output, Power in this case. Polarization curve is another key input for fuel cell sizing and stack design. Polarization curve best describes the unit cell performance. Various operating parameters determine the fuel cell performance like reactant gases pressure, flow rates, cell temperature and humidity. These operating conditions are decided based on application requirements.

Based on the guidelines available in literature, I obtained the size of the fuel cell stack by calculating the number of cells needed to deliver my desired power and voltage levels.

The cell voltage is chosen to 0.6 V based on the general voltage-current density graph available in literature [3, 6]. For our specific application, the required voltage is 24 V. The number of cells will be; $NumberofCells = 24/0.6 = 40$

The total current from the stack when supplying the maximum power can now be calculated.

$P = U.I \Longrightarrow I = P/U$

$= 200/0.6x40$

$= 8.33A$

Where,

P = Power [W]

U = Voltage [V]

I = Current [A]

For a specific power rate, the current can be increased or decreased, depending on the need of the load, if the voltage is altered by changing the number of cells. If the needed voltage is different from the stack voltage, a voltage regulator could be used to achieve the right level.

From Voltage-Current Density curve available in literature [3, 6], it can be found that the current density for 0.6 V is around $450mA/cm^2$. The area of each cell can now be calculated using the current calculated by using following equation.

$A = I/J$

$= 8.33/.45$

$= 18.51cm^2$

Where,

$A = Fuelcellarea[cm^2]$

$J = Currentdensity[A/cm^2]$

The total size of the stack depends on this area, the number of cells and the thickness of each cell. For simplicity, I selected $20cm^2$ area and designed my fuel cell.

2.2 Mechanical Model of PEM Fuel cell components

2.2.1 Bipolar Plates

Bipolar plates are one of the critical components to be designed in terms of functional, physical and durability requirements. Most of the weight and volume of the fuel cell stack is contributed by Bipolar plates, therefore it is desirable to design and fabricate plates with the smallest possible dimensions especially the thickness (< 3 mm in thickness) [1]. Reactant gas flow channels are engraved on each side of the plate, for fuel and oxidant respectively. Fuel side where traditionally Hydrogen is supplied is called Anode while flow fields for Oxygen or Air flow is called Cathode. Membrane Electrode Assembly (MEA) which will be explained in a later section is sandwiched between two bipolar plates. Gasket or seal is also provided between the bipolar plate and MEA for reactant gases leakage prevention. This make up a unit cell, several unit cells are serially joined to build fuel cell stack.

2.2.1.1 Main Functions of Bipolar Plate

Bipolar plates must perform a number of critical functional requirements efficiently. The are responsible for stack performance and durability. Following are some of the important functions performed by BPPs [6].

1. BPPs connect individual cells together electrically.
2. Supply the reactant gases to the membrane electrode assembly through flow channels engraved, facilitating the gases to react properly.
3. They are the strongest parts in a cell and provide support to the thin,flexible and mechanically weak MEAs
4. Bipolar plates facilitate water management via fuel flow channels.
5. Sometimes separate dedicated cooling plates are provided within the unit cell for extra heat dissipation, In case of absence, the BPPs also facilitate heat management. BPP material and flow field design facilitate these functions. Several flow channel designs have been reported in literature like serpentine, parallel flow and

inter-digitated. The purpose can also be served through internal manifolds, humidification and integrated cooling. Again, the optimal design have to be researched due to other fuel cell conflicting requirements.

2.2.1.2 Essential Requirements

Following listed requirements are essential for Bipolar plates in terms of Physical and Chemical characteristics.

1. Uniform distribution of the reactant gases
2. Excellent electronic conductivity
3. Good mechanical strength
4. Impermeability to reactant gases
5. Resistance to corrosive cell environment
6. Low cost and light weight in terms of material
7. Easy to manufacture in terms of cost and manufacturing time

2.2.1.3 Gas Flow Channel cross-section and layout design

1. Rectangular fluid flow channels cross-section is preferred in terms of ease of fabrication and performance. Many other cross-section designs have also been studied in detail and their pros and cons are explored like trapezoidal, triangular, semi circular, etc. [7].
2. The flow channel width and depth have been reported to be best in the range 1 to 2 mm for a appropriate fluid pressure loss due to friction.
3. Engraving or milling of flow channels on BPP are commonly used fabrication methods. Graphite or metal plates are machined to create flow field designs on both sides for Anode and Cathode respectively.
4. Optimum channel depth, width and land areas of 1.5, 1.5 and 0.5 mm respectively have been reported in literature through simulations and experimentation. Kumar

et al., in a study showed that "decreasing land width will increase hydrogen concentration at the anode, further triangular and hemispherical cross sections have land dimensions close to zero" [8].

According to Gamburzev [9], One of the main hindrance to mass producing the fuel cell bipolar plates is the gas flow channels, including the cost effective and light weight materials development, design optimization and manufacturing techniques. The largely impact on PEM fuel cell performance, the energy efficiency and power. Watkins et al. have reported that upto fifty percent output power density increase can be obtained just by appropriate distribution of gas flow channels alone [10, 11]. Li et al. summarize traditional gas flow channel geometrical configurations and a variety of different designs. They typically consist either pin, straight or serpentine type of flow field channels [12]. Many other types of alternate designs have been proposed by researchers and fuel cell developers. Following are a few most commonly used;

1. Pin type flow field,
2. Series / parallel flow field,
3. Single or multiple Serpentine flow field,
4. Integrated flow fields,
5. Inter-digitated flow field,
6. Flow designs made of metal sheets.

For my fuel cell, I selected double serpentine flow field pattern. This design selection was made based on fluid flow simulations which will be detailed in Chapter 3. The model drawn in SolidWorks is shown in Figure 2.1 as Anode side while in Figure 2.2 as Cathode side.

2.2.2 Membrane Electrode Assembly

The three-layer Membrane Electrode Assembly (MEA) can be considered as the heart of PEM fuel cell. Proper functioning of fuel cell is dependent on electrolyte. In a PEM fuel cell the fuel, Hydrogen in this case, makes a contact with the catalyst layer and split

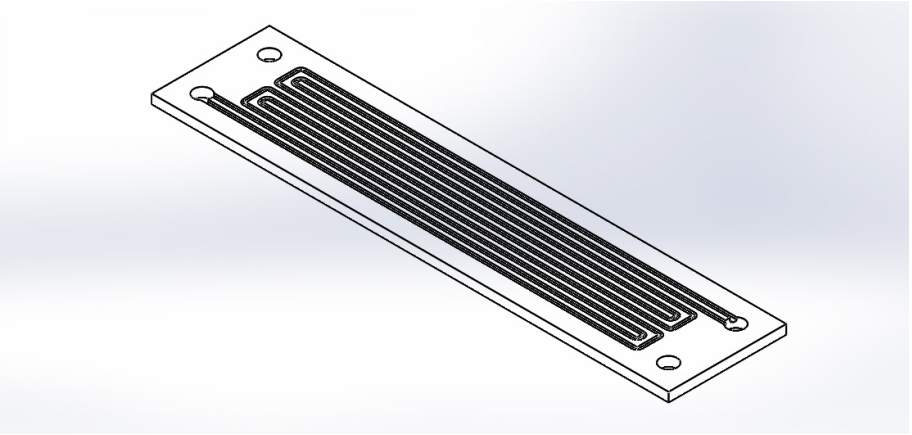

FIGURE 2.1: Bipolar Plate - Anode side

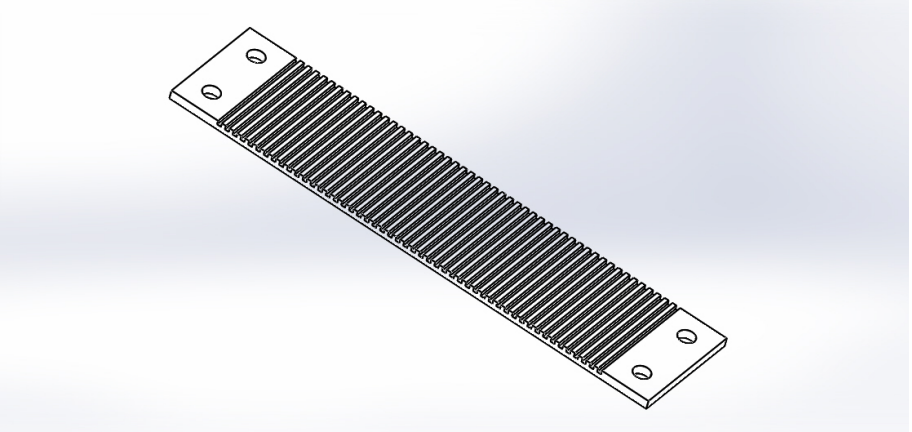

FIGURE 2.2: Bipolar Plate - Cathode side

up into protons (H^+) and electrons e^-. The electrons travel to the outer circuitry to give electric current, and the Hydrogen protons diffuse through the electrolyte to reach the Cathode side and react with Oxygen to form water. Heat is also produced as a by-product during the chemical reaction. The PEM fuel cell electrolyte layer must posses following essential properties in order to work fuel cell properly:

1. Posses high ionic conductivity
2. Offer an appropriate barrier to the reactant gases
3. Must show stability, both chemically and mechanically
4. Posses low electronic conductivity
5. Easy to manufacture / easily available
6. Low cost

Currently, co-polymer of poly-tetra-fluoro-ethylene and poly-sulfonyl-fluoride vinyl ether are being used as the standard electrolyte materials in PEM Fuel Cells. The most commonly electrolyte used in PEM fuel cells is developed by DuPont company and is generally known with the name "Nafion". The Nafion membranes are quite stable in strong basic chemical environment, strong oxidizing and reducing acid environments like, $H_2O_2, Cl_2, H_2, and O_2$ at high temperatures.

Schematic SolidWorks model is shown in Figure 2.13 representing 3-layer Membrane Electrode Assembly.

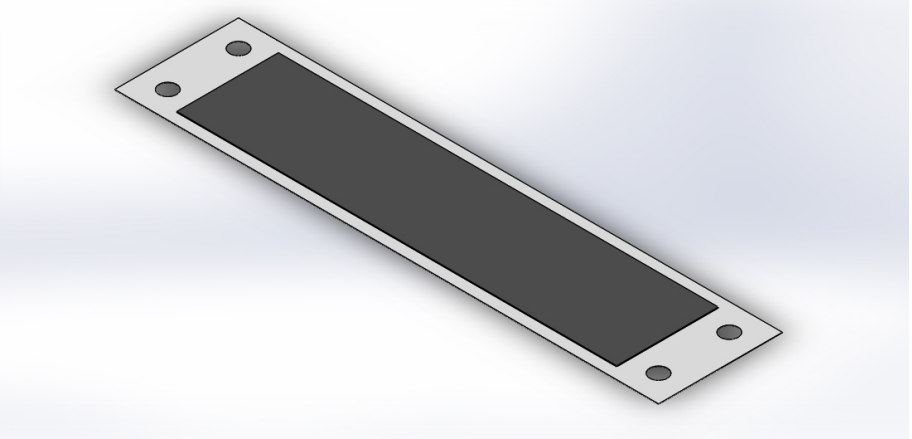

FIGURE 2.3: 3-Layer Membrane Electrode Assembly

2.2.3 Gas Diffusion Layer

The gas diffusion layer (GDL) is provided between the catalyst layer and the bipolar plates. In a PEM fuel cell, the catalyst, gas diffusion layer and polymer membrane layers (also known as membrane electrode assembly (MEA)) are sandwiched between the bipolar flow field plates. The gas diffusion layer provides following five important functions for a PEM fuel cell:

1. Assure electronic conductivity
2. Provide Mechanical support for the proton electrolyte membrane
3. Act as a porous media for the catalyst to facilitate reactant gases access
4. Product water removal from the cell to avoid membrane flooding

Gas diffusion layer is made up of a porous and highly electrically conductive material. The most commonly used GDL materials are carbon cloth and carbon paper. Properties like thickness, porosity and density are of most concern while selecting a GDL. Some of the commercially available carbon papers are listed below.

1. Toray TGPH 090
2. Kureha E-715
3. Spectracarb 2050A-104
4. AvCarb Gas Diffusion Systems

The key function of a GDL is to facilitate water in PEM fuel cell in an appropriate amount to contact the membrane/electrode assembly and keep the membrane humidified. Moreover, it helps manage the exit of liquid water from the Cathode side to avoid membrane flooding. A simple model drawn in SolidWorks with designed dimensions is shown in Figure 2.4

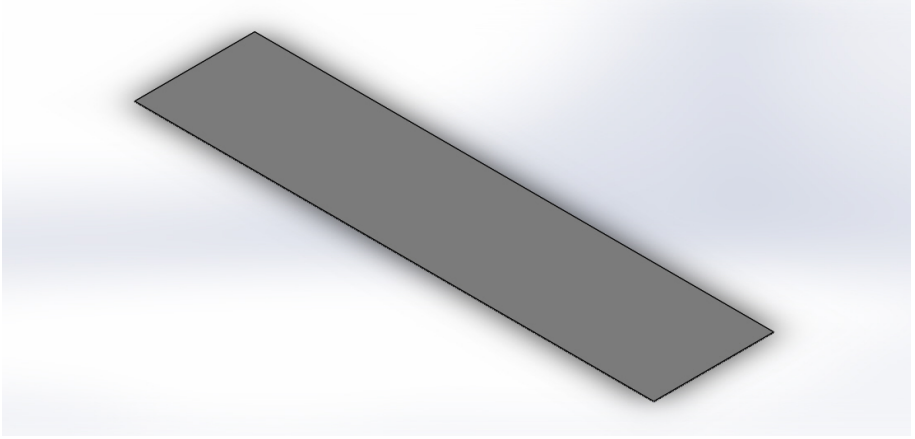

FIGURE 2.4: Gas Diffusion Layer (GDL)

2.2.4 Seal / Gasket

The purpose of seal / Gasket in PEM fuel cells is to prevent leakage of reactant gases. This component is also very critical in terms of PEM fuel cell performance. Thickness of gasket should be calculated with great care as the inappropriate thickness may tremendously affect cell performance. Over defined thickness can result inappropriate contact between the bipolar plate and MEA while under defined thickness may result

over compression of GDL and MEA that promote mechanical failure. In both cases fuel cell performance will decrease as well as can cause degradation issues. Seal cut to size with the designed dimensions is shown in Figure 2.5.

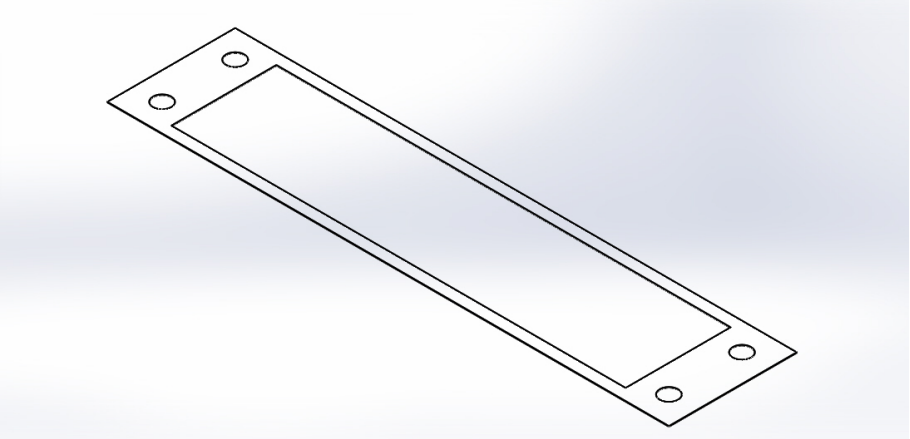

FIGURE 2.5: Seal / Gasket

2.2.5 End Plates

Xinting et al. [13] studied comprehensively the end plate design and compaction pressure effects on fuel cell performance. In a traditional PEM fuel cell design, end plates are the two outermost components in a stack assembly. They are used to clamp a number of unit cells together and provide sufficient compressive force to make proper contact between the components. Main functions of end plates can be summarized as below;

1. To ensure good electrical contact between multiple layers.
2. To ensure good sealing at various interfaces.
3. To provide passages for the reactants, products and possibly cooling agents to enter and leave the fuel cell.
4. In some cases, to provide electrical leads for connections to external loads.

For my fuel cell, I selected Aluminum as end plates material for ease of manufacture and low cost. Variety of other materials can be used for end plates but design is important and it should serve the functions mentioned above. SolidWorks drawing generated is shown in Figure 2.6.

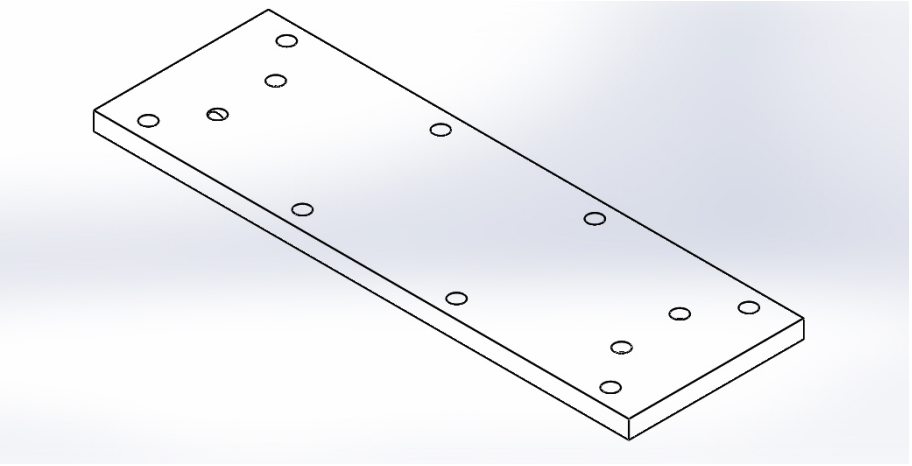

FIGURE 2.6: End Plate

2.2.6 Single Cell Assembly

After getting all the components manufactured, they are assembled to make individual cells. Subsequently, a number of cells are connected in series to get the required voltage level. Generally, fasteners are used to join the cells between two end plates. A schematic diagram drawn in SolidWorks for my design as an exploded view is shown in Figure 2.7.

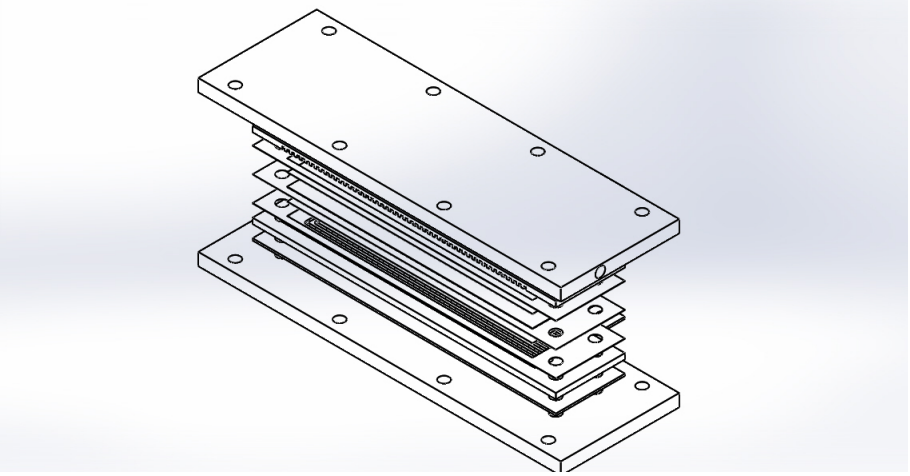

FIGURE 2.7: Single cell assembly - exploded view

2.3 Prototype Fabrication

2.3.1 Bipolar Plates

As a first step, I selected the most commonly used Graphite material to fabricate bipolar plates. CNC milling machine was used for cutting the Graphite sheets to size and creating gas flow channels on each side. I used the machining facility of Nanotechnology Research center at Gebze Technical University . CNC milling with Mach3 control used for bipolar plates fabrication is shown in Figure 2.8.

FIGURE 2.8: CNC Milling for machining components

Finished bipolar plate is shown in Figure 2.9 as Anode side with serpentine flow channels and Figure 2.10 as Cathode side with straight through channels.

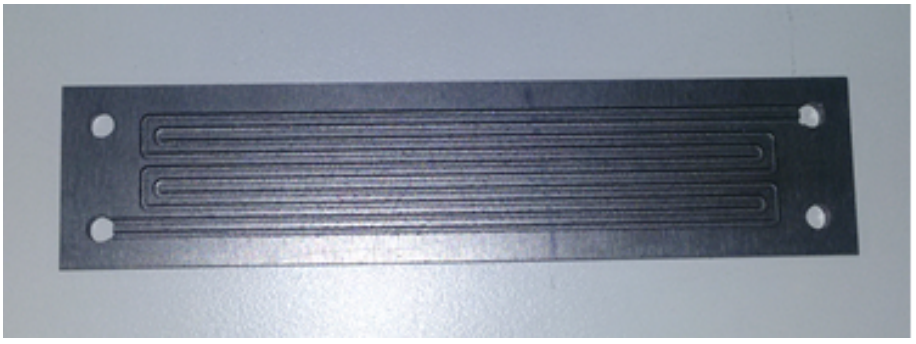

FIGURE 2.9: Bipolar Plate - Anode Side

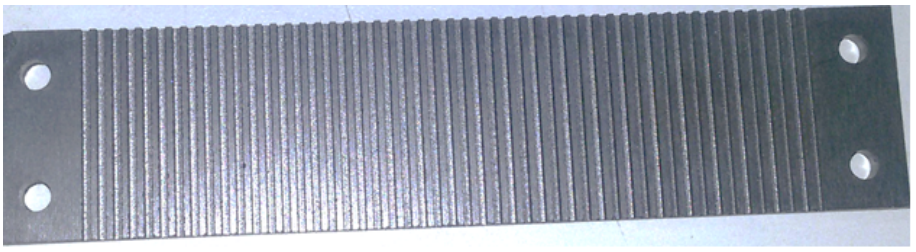

FIGURE 2.10: Bipolar Plate - Cathode Side

2.3.2 Membrane Electrode Assembly (MEA)

For my specific fuel cell stack, I selected commercial Nafion-XL membrane and Tanaka catalyst with 38 wt% Pt/C composition and prepare MEAs. Screen printer and decal transfer process was used to deposit catalyst layer on Nafion membrane. Firstly, Catalyst paste like material was prepared and coated on Teflon sheets by an ATMA AT-45 PA semi-automatic screen printer shown in Figure 2.11. Both Anode and cathode catalyst layers were prepared with a platinum loading of $0.45mg.cm^{-2}$. The coated Teflon sheets were then sandwiched between a Nafion-XL membrane and placed in a hot press. The components was compressed up to 150 bars at $130°C$ for approximately 8 minutes. The catalyst layers were transferred on the membrane and the Teflon sheets were peeled off. Multiple MEAs were prepared with the same procedure and conditions to ensure repeatably. The active areas of the MEAs were $20cm^2(10cmx2cm)$

During the MEA preparation process, the catalyst applied on Teflon sheet is shown in Figure 2.12. Afterwards, catalyst transferred on Nafion is shown in Figure 2.13. Finally, Gas diffusion layer was cut to dimensions as that of catalyst layer and put on both sides of membrane forming a complete Membrane Electrode Assembly (MEA).

2.3.3 Single cell assembly

After all the components get manufactured, a single cell assembly was prepared. Eight (8) bolts were used to fasten the cell assembly and appropriate torque was applied in a sequence. Gas inlet and out valves were installed on End plate. Since my fuel cell stack was designed as an air-breathing system, a small fan was fixed on the cell to provide sufficient air to the Cathode. Single cell assembly without fan installed is shown in Figure 2.14 and with air supply fan fixed is shown in Figure 2.15.

FIGURE 2.11: Screen Printer

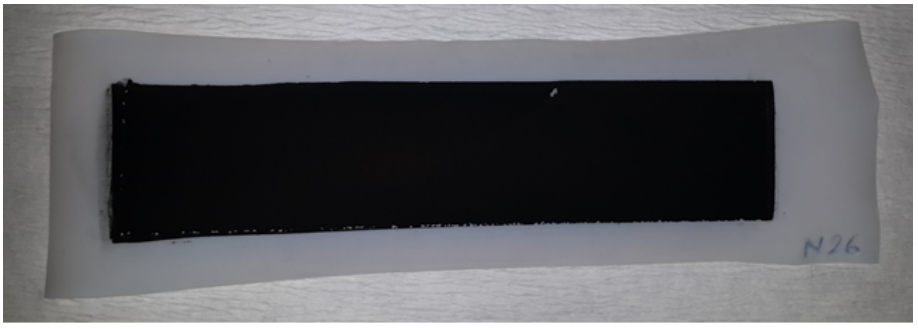

FIGURE 2.12: Catalyst on Teflon Sheet

FIGURE 2.13: Membrane with Catalyst Layer deposited

FIGURE 2.14: Single cell Assembly without air blower

FIGURE 2.15: Single cell Assembly with air blower

Chapter 3

Development of PEM Fuel Cell using simulated results of bipolar flow field design and electrochemical models

3.1 Introduction

Polymer Electrolyte Membrane (PEM) fuel cell is an electro-chemical processing device similar to battery which transform chemical energy stored in fuels, Hydrogen in this case, to electrical energy directly. In its typical operation, the fuel (hydrogen in this case) is supplied to one electrode called Anode, and Oxygen or air to other electrode called Cathode. Hydrogen split up into Protons and electrons by the action of Catalyst at Anode. Protons travel to the cathode through the electrolyte and react with Oxygen at Cathode to form water and dissipate heat as well. While electrons travel through the outer circuit producing useful electrical energy. Instead of Hydrogen, many other types of fuels can also be fed to PEM fuel cell. For example ethanol and biomass derived materials. These fuels can be directly supplied to the fuel cell, or supplied to a reformer first to get pure Hydrogen. And this is then directly supplied to the fuel cell. The Hydrogen (H_2) and oxygen (O_2) have a capability to chemically react together strongly and provide electrical energy to power up any system directly. Moreover, fuel cell devices

produce clean electrical energy unlike Internal Combustion Engines (ICEs). Many single cells can be joined together to make a fuel cell stack in order to fulfill the desired output power. Another important aspect is, the PEM fuel cell can operate at low temperatures, typically ranging from 50 to 80 $^{\circ}C$, and are very safe in applications.

However, to make fuel cells commercially practical, it is necessary to make improvements in fuel cell efficiency, reduce material and manufacturing costs and increase reliability and durability of its individual components. Membrane Electrode Assembly (MEA) and Bipolar Plates (BPPs) are the potential components to be worked on for achieving these improvements. The BPPs contribute towards the major portion of fuel cell weight and volume. It is worth mentioning that bipolar plates constitute about 80 percent of volume of the fuel cell system. [14, 15]. Bipolar plates must be vulnerable to chemically corrosive environment and strong enough for mechanical forces they have to bear during gas flow channel machining and assembly processes [16–22]. Non porous graphite is the most commonly used material which shows high chemical stability and high conductivity for heat and electrons. Its brittleness and costly manufacturing are main disadvantages. Other competitive materials are metals and their alloys such as aluminum, iron as reported by Fleury et al. [23] stainless steel as studied by Wang et al. [24–26] titanium and nickel by Silva et al. [27]. polymer composites are also a good candidate as mentioned by Huang et al. and others, [28, 29] silicon, [30]. Moreover, carbon-based materials as experimented by Wang et al. [31] are also a good low cost solution. Over the recent years, Expanded graphite (EG) and its polymer composites have been extensively studied. They highly competitive alternate to worldly used natural graphite as reported by several authors like Du et al., Dursun et al, etc. [32–39]. The most important advantages of expanded graphite - epoxy composite bipolar plates are their low density and manufacturability at low thicknesses as highlighted by Du et al., Xu et al., Dhakate et al., and many others [32, 35–39]. These composites can lead to dramatic improvements in PEM fuel cell stack especially in terms of weight and volume reduction [16, 40].

3.2 Simulations

3.2.1 Bipolar Plate fuel flow channel simulations

Bipolar plates are provided with flow channels to feed and uniformly distribute Hydrogen and Oxygen at Anode and Cathode respectively. They also provide a path for byproduct water removal. Typically, flow channels are engraved within the BPPs with a cross sectional dimensions of around 1 mm. In-sufficient supply of reactants gases may cause fuel starvation which consequently result in reducing cell performance and durability. The fuel flow fields must allow minimum gas pressure drop in order to reduce parasitic pump requirements. Evenly mass transfer distribution, effective water management and ease of manufacture must also be considered while designing the flow fields. Wang et al., Li et al., and several authors have reported different types of flow channels in literature and highlighted their pros and cons. They have already been mentioned briefly in chapter 2, Bipolar plate section [41, 42]. Jiang et al., reported a zig-zag type of flow field [43]. Jeon et al., [44] proposed single channel, double channel, cyclic single channel, and symmetric single channel fixtures and concluded fuel cell performance variation in different configurations. Many other studies also put their efforts to investigate the cross-section dimensions of flow fields. Inoue et al. [45] examined channel height and found that shallow channels may enhance oxygen transport to electrodes.

In this study, keeping in view the space limitations, rectangular bipolar plate was designed with five different channel shapes using SolidWorks modelling software. As air breathing system was designed, cathode side of bipolar plate was made with parallel flow channels, 1mm wide, 1mm height and 1mm as the distance between channels (land area). Only Anode side was considered for fluid flow analysis. All the channel shapes were engraved 1mm in width, 1mm in height. The distance between two consecutive channels (land area) was also 1mm. Models generated in SolidWorks were exported to ANSYS Fluent for fluid flow analysis. Mass flow rate was calculated to be $2.5x10^{-7}$ kg/s corresponding to the active area. The mass flow of hydrogen entering the bipolar plate was $2.5x10^{-7}$ kg/s at 1 atm pressure and is at a temperature of 333 K. For simplicity, I assumed that a fix mass flow of Hydrogen being exited at the BPP Anode. It is worth mentioning that, in a real system the Hydrogen mass flow reduces as it flows down-stream. Because, the hydrogen flow rate is directly linked with the electrical

current in the fuel cell. Hence, the method applied here will only show a conservative estimate of the pressure drop. Outlet was set as outlet-vent at 1 atm. Same meshing parameters and boundary conditions were applied on all five designs for their comparison. With area-weighted average monitors, static and dynamic pressure distribution, and velocity distributions were obtained and compared. The best design with minimum pressure drop, with optimal water management and easy to manufacture was selected. The ANSYS analysis results showing static pressure drop and velocity vector profiles are presented from Figure 3.1 to Figure 3.10 below. Based on the simulation results, design 2 (Figure 3.3 and 3.4) was selected for fabricating the prototype.

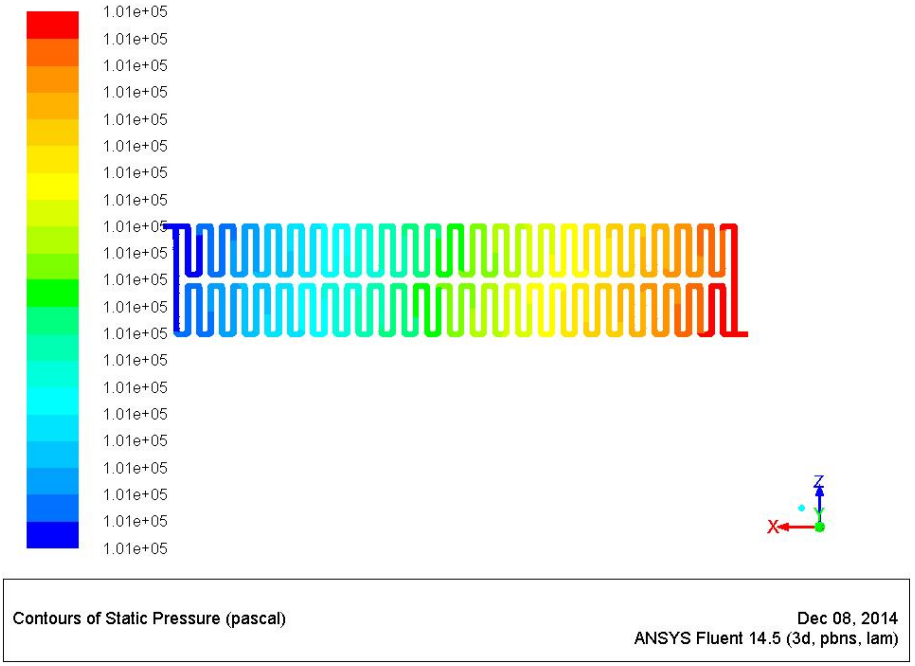

FIGURE 3.1: Static pressure distribution - DS vertical

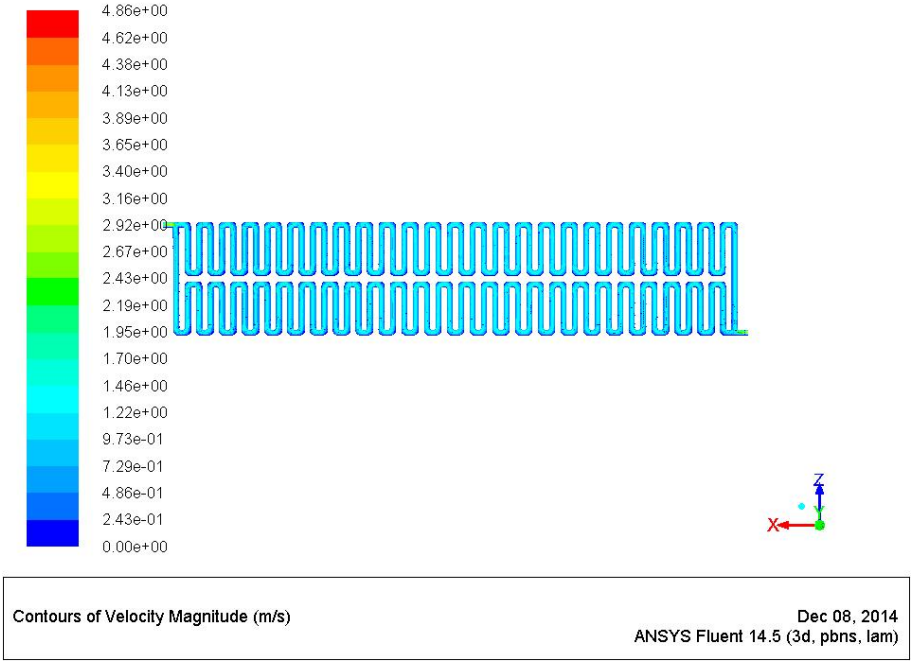

FIGURE 3.2: Velocity Vector distribution - DS vertical

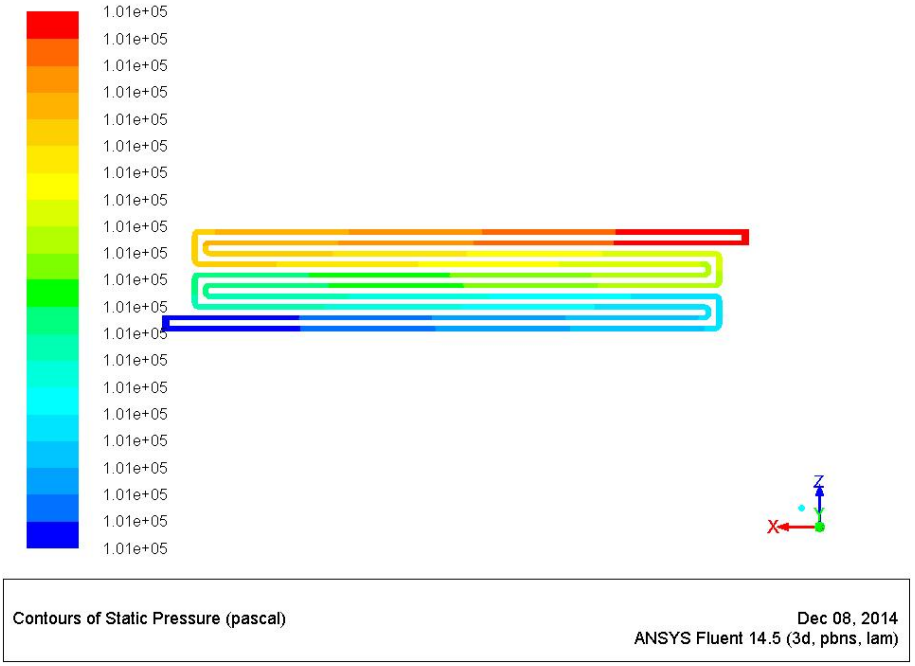

FIGURE 3.3: Static pressure distribution - DS Horezontal

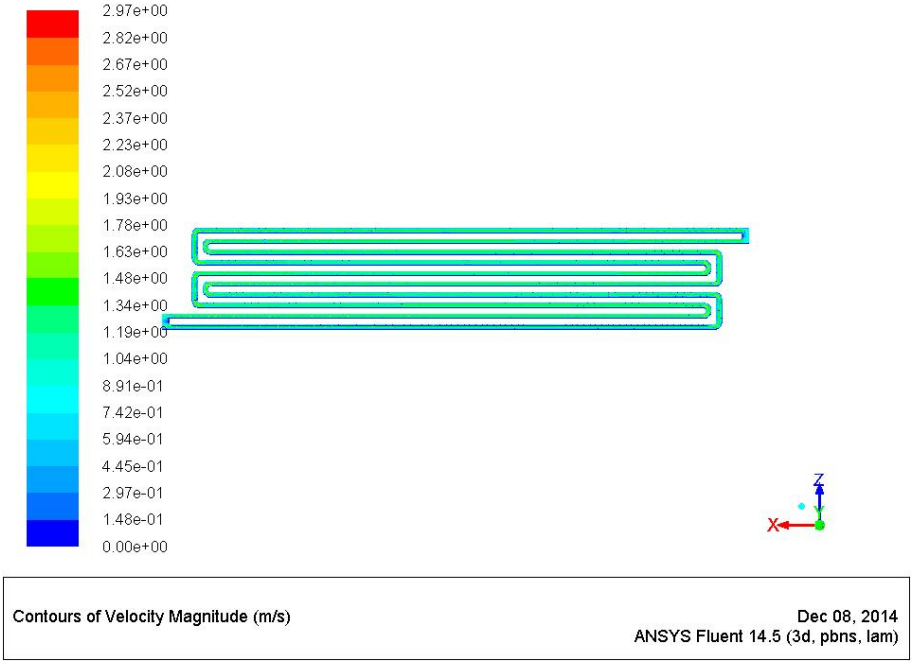

FIGURE 3.4: Velocity Vector distribution - DS Horezontal

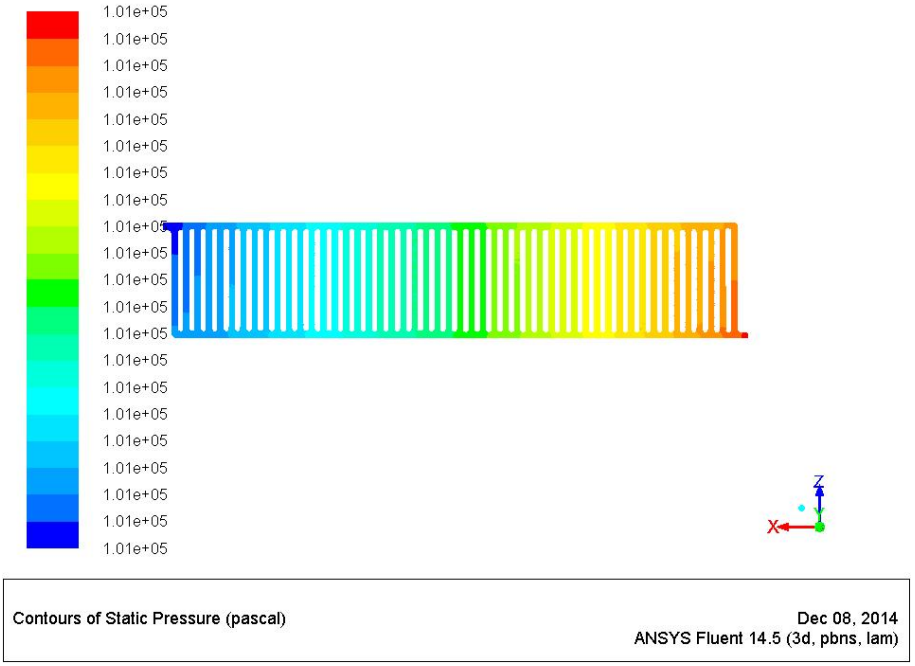

FIGURE 3.5: Static pressure distribution - Parallel Flow

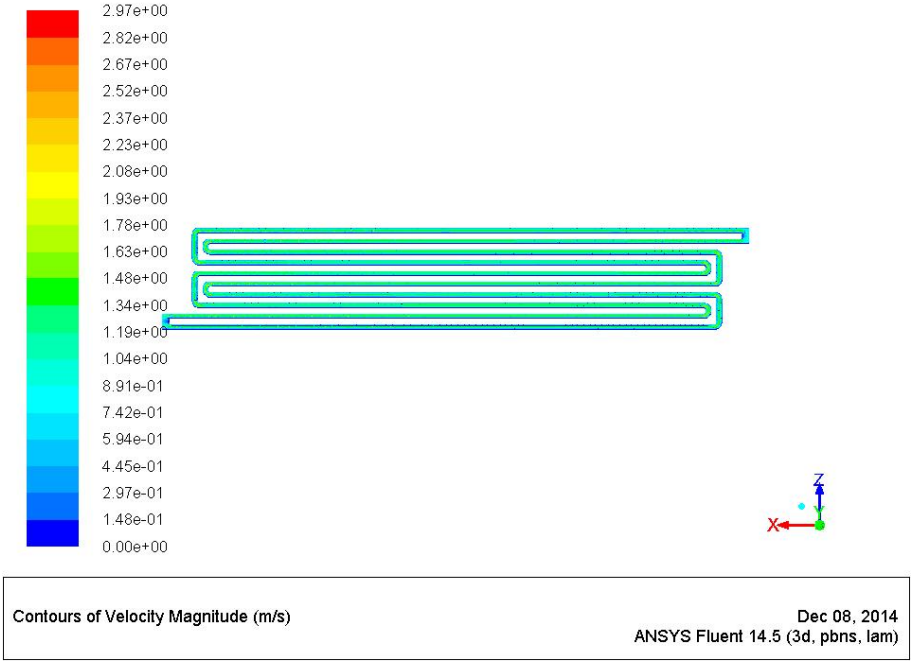

FIGURE 3.6: Velocity Vector distribution - Parallel flow

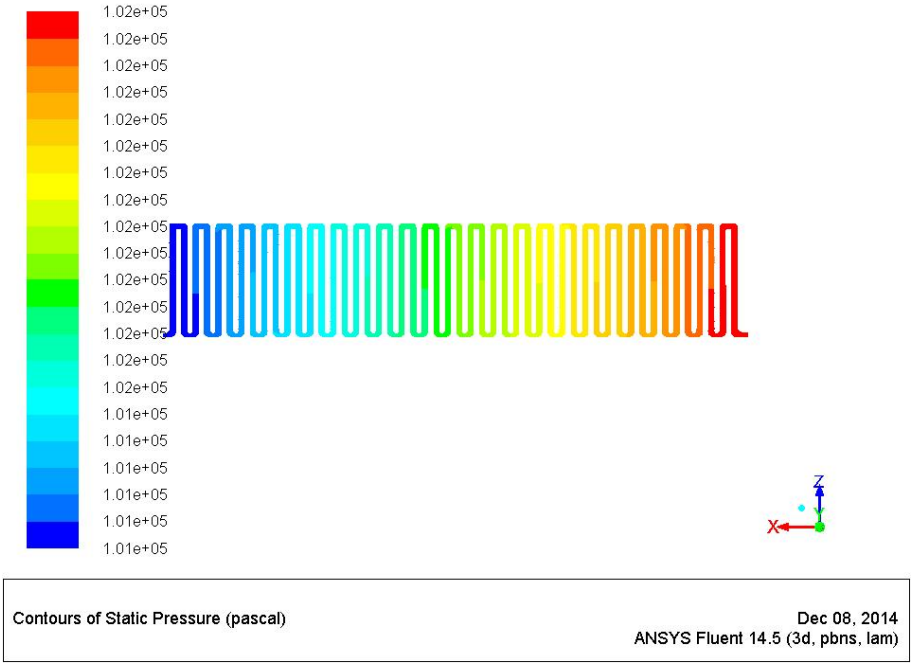

FIGURE 3.7: Static pressure distribution - Single vertical

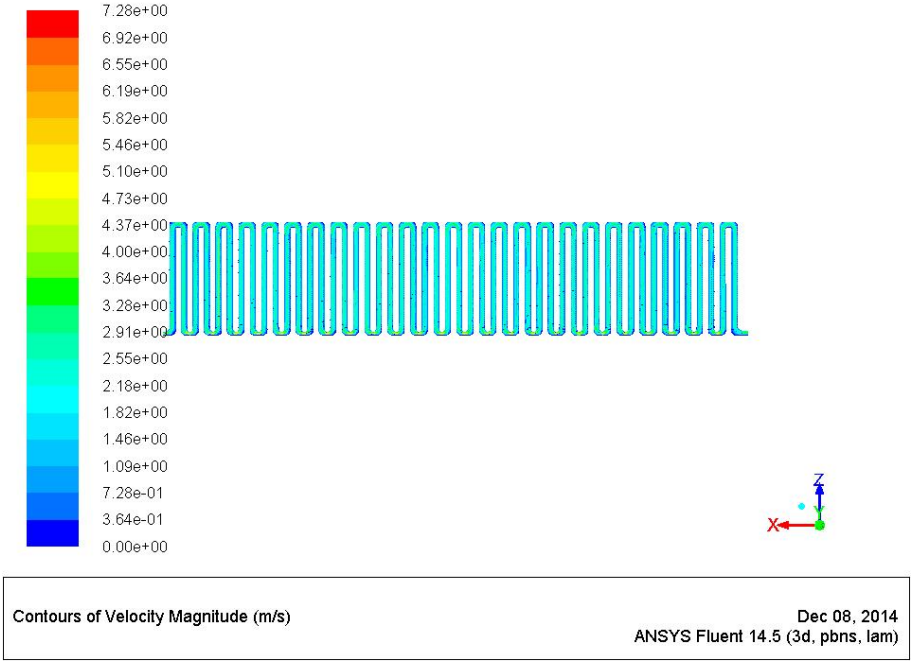

FIGURE 3.8: Velocity Vector distribution - Single vertical

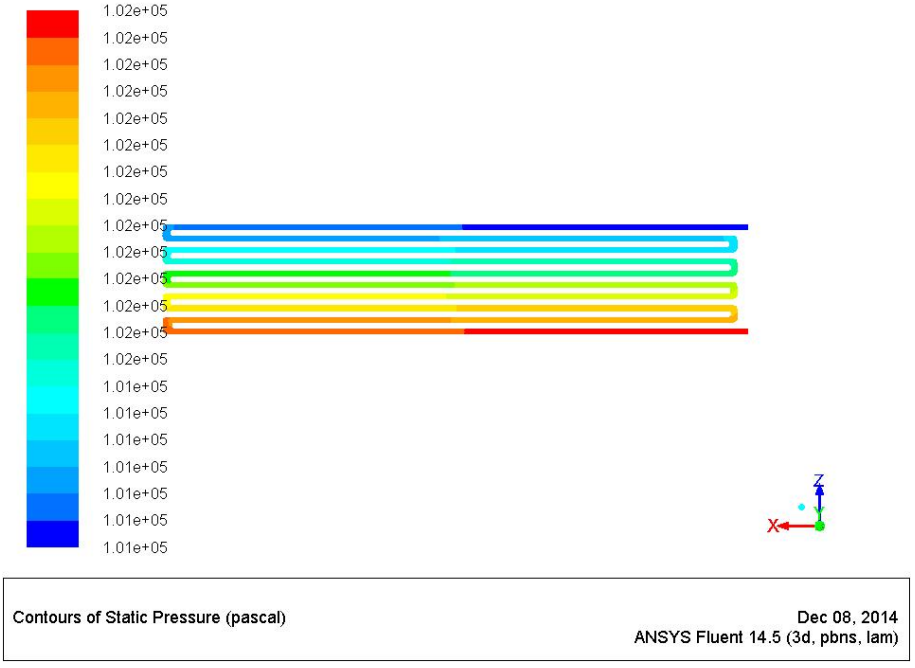

FIGURE 3.9: Static pressure distribution - Single horezontal

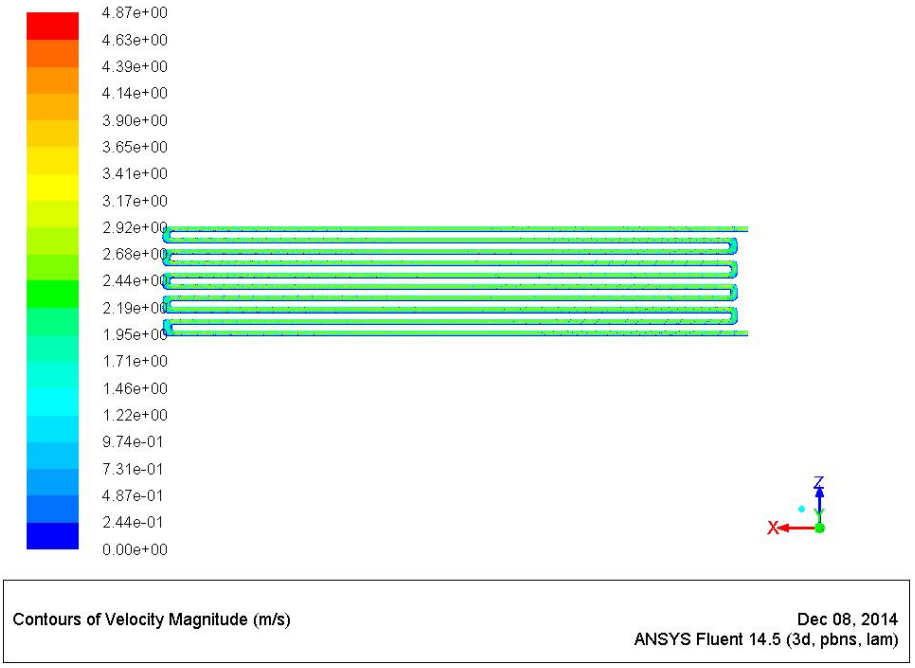

FIGURE 3.10: Velocity Vector distribution - Single horezontal

3.2.2 Electrochemical simulations for Performance Prediction

Modeling and simulation are the best engineering approaches for checking the system response to input parameters without manufacturing the actual system. This approach allows a lot of benefits including cost, time and system flexibility to make changes. For designing a fuel cell, it is essential to understand the chemical reactions and processes occurring at the anode and cathode. The electrochemical reactions control the rate of power generation. A number of studies have been made to explain electrode kinetics, but there is still need to explore and develop solutions in order to understand the actual complex anode and cathode kinetics. Several mathematical models of PEM fuel cell have been reported in the literature [46]. For this study, the fuel cell model proposed by Amphlett et al. [47] was considered. The output voltage of a single fuel cell can be defined as [48].

$$U_{cell} = E_{Nernst} - U_{act} - U_{\Omega} - U_{con} \tag{3.1}$$

where U_{cell} (V) is the fuel cell output voltage at a certain operating condition, E_{Nernst} (V) is the reversible voltage; U_{act} (V) is the voltage drop due to the activation of the anode and cathode; and U_{Ω} and U_{con} (V) are the ohmic and concentration voltage drops, respectively. In order to generate required amount of power, a number of single fuel cell

can be assembled into a fuel cell stack system.

$$U_S = n.U_{cell} \tag{3.2}$$

where U_s is the stack voltage and n is the number of cells connected in series in the stack.

1. Reversible voltage E_{Nernst}

   A form of the Nernst equation is used since it allows to investigate the performance in view of temperature, system pressure, and the particle pressure of both hydrogen and oxygen. It can be obtained by Ref. [49].

$$E_{Nernst} = 1.229 - 0.85x10^{-3}.(T - 298.15) + 4.3085x10^{-5}T.(ln(P_{H2}) + 0.5.(ln(P_{O2})) \tag{3.3}$$

   where T (K) is the cell operation temperature; P_{H2} and P_{O2} are the effective partial pressure (atm) of Hydrogen and Oxygen, respectively and can be calculated as follows,

$$P_{O2} = RH_c.P_{H2O}.[(exp(4.192.((i/A))/T^{1.334}).(RH_c.P_{H2O})/P_c)^{-1}] \tag{3.4}$$

$$P_{H2} = 0.5.RH_a.P_{H2O}.[(exp(1.635.((i/A))/T^{1.334}).(RH_a.P_{H2O})/P_a)^{-1}] \tag{3.5}$$

   where RH_a and RH_c are the relative humidity of vapor in the anode and cathode; P_a and P_c are the anode and cathode inlet pressure (atm); i (A) is the cell operating current; A is the activation area of the membrane, and P_{H2O} represents the saturation pressure of the water vapor (atm), which can be expressed as a function of the cell temperature (T) [50] [37].

$$Log(P_{H2O}) = 2.95x0.01.(T - 273.15) - 9.18.10^{-5}x(T - 273.15)^2$$
$$+1.44.10^{-7}.(T - 273.15)^3 - 2.18$$

2. Activation voltage drop U_{act}

   U_{act}, which is caused by the sluggish reaction of the reactants, can be expressed as follows [36].

$$U_{act} = -[(\xi_1 + \xi_2.T + \xi_3.Txln(CO_2) + \xi_4.ln(i)] \tag{3.6}$$

   where $\xi_1, \xi_2, \xi_3, and \xi_4$ are parametric coefficients for each cell model. The values of these parameters are defined based on mathematical equations with kinetic, thermodynamic and electro-chemical foundations; CO_2 is the concentration of dissolved oxygen (mol/cm_3) on the interface of the cathode catalyst, which can be calculated by Henry's law expression as follows,

$$CO_2 = PO_2/(5.08.10^6.e^{-(498/T)}) \tag{3.7}$$

3. Ohmic voltage drop U_Ω

   The ohmic voltage drop is the potential drop due to the equivalent membrane resistance R_M, contact resistance R_C between the membrane and electrodes, as well as the electrodes and the bipolar plates. It can be obtained by using the Ohm's law as follows,

$$U_\Omega = i.(R_M + R_C) \tag{3.8}$$

   Further, according to Ohm's law, the equivalent resistance of the membrane R_M can be calculated as

$$R_M = (\rho_M.l)/A \tag{3.9}$$

   where l is the thickness of the membrane (cm); ρ_M is the specific resistivity of the membrane for the electron flow ($\Omega.cm$), which can be obtained by the following

numeric expression.

$$\rho_M = (181.6.[1 + 0.03.(i/A) + 0.062.(T/303)^2.(i/A)^{25}])/((\lambda - 0.634^{-3}.(i/A)) .exp[4.18.((T - 303)/T)])$$

where λ is the water content of the membrane, which is an adjustable parameter from a possible maximum value.

4. Concentration voltage drop U_{con}
   Concentration voltage drop is caused by the mass transportation, which affects the concentrations of hydrogen and oxygen. It can be determined by,

$$U_{con} = -b.ln(1 - J/J_{max}) \tag{3.10}$$

where b is a parametric coefficient (V) that depends on the cell and its operation condition. J is the actual cell current density (A/cm^2), and J_{max} is the maximum value of J.

$$J = i/A \tag{3.11}$$

With above formulations, the PEM fuel cell stack model can be built up easily. As long as the seven unknown parameters (ξ_1, ξ_2, ξ_3, and ξ_4, l, b, RC) are determined, the output US corresponding to a certain input i can be predicted immediately. ANSYS, MATLAB Simulink and some other customized software are being used for Electro-chemical simulations of fuel cells. We used MATLAB for performance prediction of PEM fuel cell. Polarization and power curves are the most popular outputs for getting an insight of fuel cell system response under given conditions. We plugged in different operating and design parameters to predict our system performance. The maximum power output of the single cell is approximately 6 watts at a current density of 450 $m.A/cm^2$ with an active area of $20cm^2$. Predicted fuel cell performance in Figure 3.11 as Polarization curve and Figure 3.12 as Power curve.

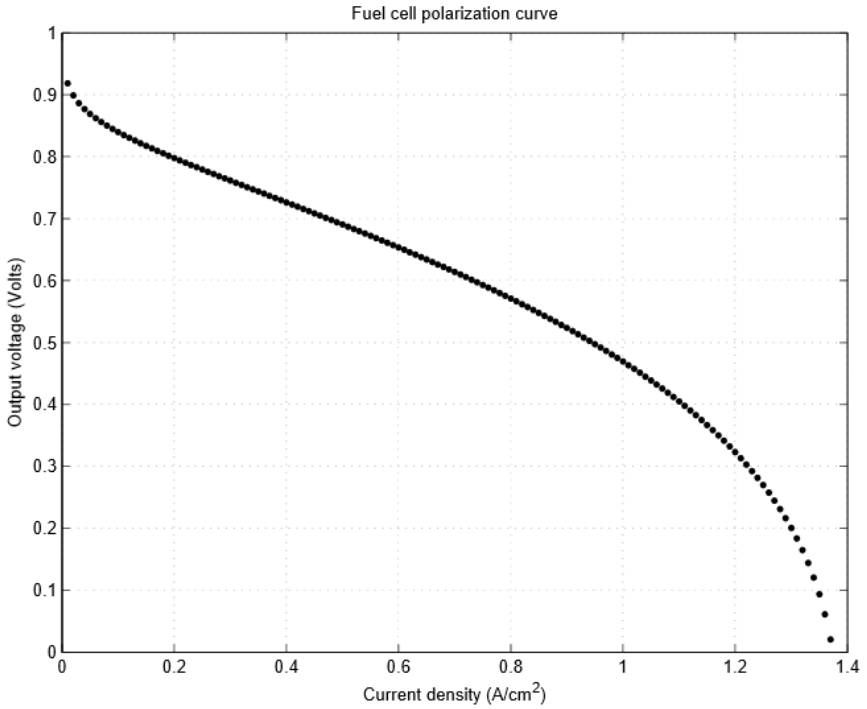

FIGURE 3.11: Performance prediction - Polarization Curve

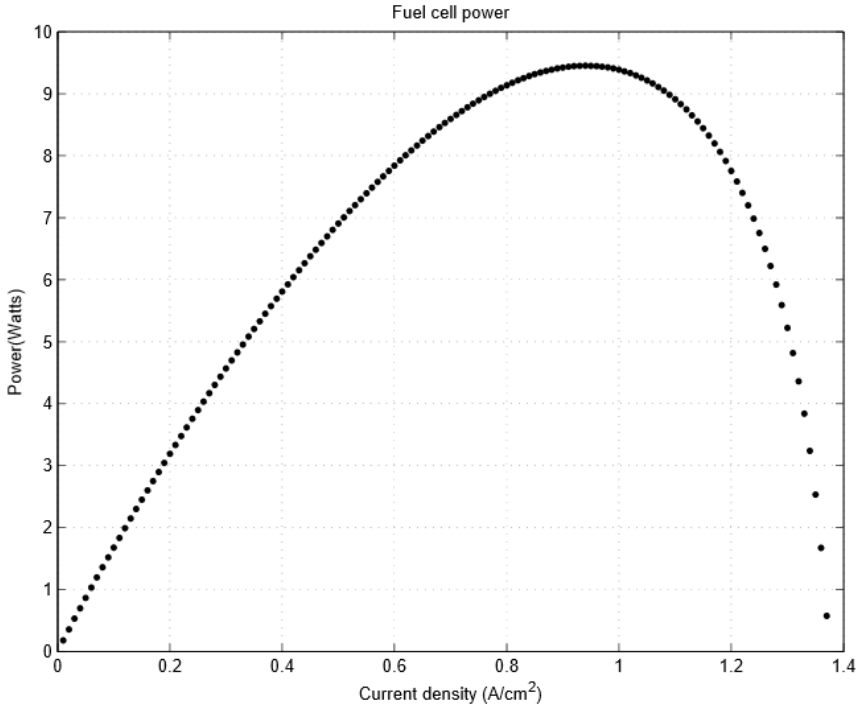

FIGURE 3.12: Performance prediction - Power Curve

3.3 Experimental

3.3.1 Materials, Method and Assembly

Graphite bipolar plates of selected design were prepared by machining. Commercially available Nafion XL membrane was selected for our fuel cell. Custom made MEA was prepared with Pt loading of $0.46mg.cm^{-2}$ and $0.42mg.cm^{-2}$ for anode and cathode respectively. Gasket thickness was calculated based on the thicknesses of membrane and GDL. Silicon Gasket with a thickness of 0.125 mm was used. Aluminum end plates were used for providing sufficient contact between the components. Copper plates with a thickness of 0.8 mm were used as current collector electrodes. Commercial Nafion XL membrane and Tanaka catalyst were used to prepare MEAs. The catalyst paste like mixture was prepared and first deposited on Teflon sheet using screen printer. It was baked in oven for a specified time to dry and then transferred on Nafion membrane by decal transfer process. The detail process has already been described in chapter 2, MEA preparation section. The active areas of the MEAs used here were $20cm_2$ (10 cm x 2 cm). Other components were also prepared as per designed dimensions with acceptable properties as defined by Department of Energy (DOE). Finally, a single cell was assembled for testing.

3.3.2 Fuel Cell Test

Finally the single cell assembly was tested for actual performance. Custom built Fuel cell test station at our labs was used for performance tests (shown in Figure 3.13. The tests were performed at $55°C$ and the reactant gases were humidified at $50°C$. Reactant gas flow rates were maintained constant (as $0.2l.min^{-1}$ and $0.4l.min^{-1}$) both for the anode and cathode respectively. The MEAs were conditioned before recording experimental results. Polarization and power values were taken after six continuous cycles. Polarization and power best describe the output of a fuel cell. The results obtained are shown in the following graphs. Although, the current and power densities are not comparable to the simulated / predicted results, however, they are a good starting point for improvement through various components. Actual fuel cell performance results obtained are shown in Figure 3.14 as Polarization curve and Figure 3.15 as Power curve.

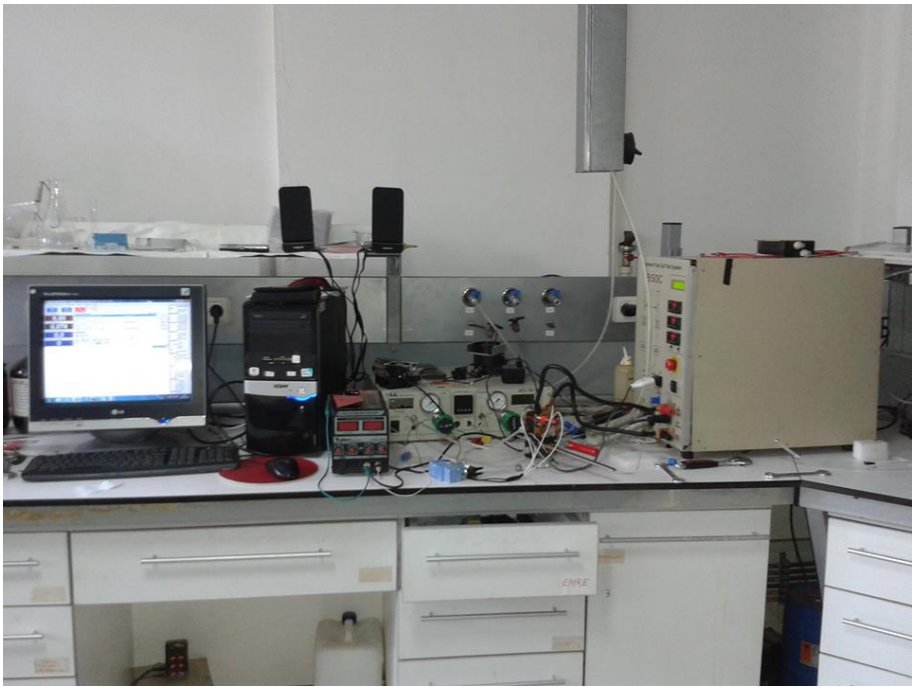

FIGURE 3.13: Fuel Cell Test station

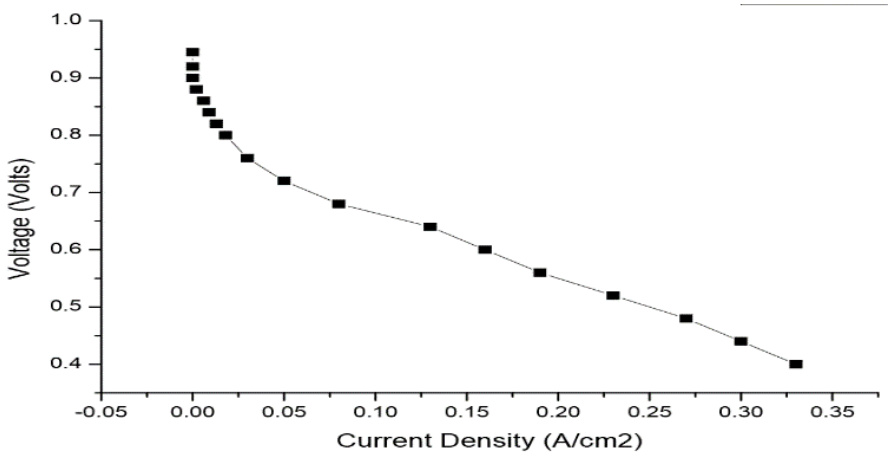

FIGURE 3.14: Fuel Cell Actual Performance - Polarization Curve

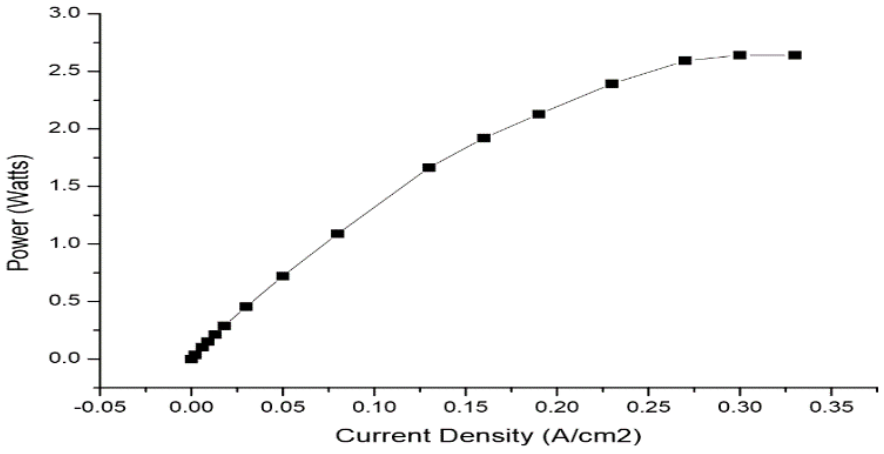

FIGURE 3.15: Fuel Cell actual Performance - Power Curve

3.4 Crux of the study

Keeping in view the space limitations, problem based study was carried out to design bipolar flow field using fluid flow analysis software (ANSYS Fluent). Five different flow field channel shapes were designed using SolidWorks and simulated using ANSYS Fluent. Static pressure distributions and velocity profiles were obtained for all design options with similar simulation parameters and compared together. Optimized bipolar design, double serpentine horizontal in this case, was selected for prototype manufacturing. Secondly, electro-chemical simulations were carried out to predict the performance characteristics of the fuel cell. MATLAB software was used to simulate the electro-chemical model and Polarization and Power curves were obtained. Finally, a prototype was manufactured for getting the actual output. Customized fuel cell components were used for making single cell assemblies. Single cell tests were performed and compared with the simulated performance results. Although experimental results were not achieved as predicted, however this study provided the insights for improvement. The cell performance can be greatly improved using high conductive bipolar plates, high conductive current collector plates and efficient MEAs.

Chapter 4

An alternate low cost fabrication technique for PEM Fuel cell bipolar plates using graphite polymer composite material

4.1 Introduction

It is already emphasized the importance of bipolar plates in previous chapters. This chapter put more effort to manufacture BPPs using alternate fabrication method with different material. Graphite polymer composite material was selected for making BPPs. Main focus was the cost and weight with improved performance, as the cost and weight of bipolar plates are the major hurdles in the way of commercialization of PEM fuel cells. United States Department of Energy (DOE) have defined yearly targets for manufacturing bipolar plates.

In order to reduce the cost of manufacturing bipolar plates, many companies have turned to graphite composites. Expanded Graphite - polymer composites were studied by several researchers. The filler content in these composites have a dramatic role in performance. High filler content is required for desired mechanical strength and gas permeability values, however it increases the electrical resistance. [51–55]. As highlighted by Spiegel et al. and Mech et al., these highly electrical conductive materials are usually compression

or injection molded producing desired fuel channel patterns. Graphite composites have several advantages over natural Graphite, like low density, greater corrosion resistance and ease of mass production. One critical performance factor is the electrical conductivity of the bipolar plate. High electrical conductivity of a bipolar plate consequently lead to reduction in number of BPPs producing the same amount of power output. This leads to a smaller fuel cell and lower cost, which are key features for market acceptance. [56, 57]. This study put an effort to fabricate light weight, low cost and high performance bipolar plates using EG - epoxy composite sheets. We devised a novel idea to manufacture bipolar plates using EG sheets. We fabricated bipolar plate by three pieces (0.6 mm each), creating anode and cathode channels on separate sheets and joining them with third one using one of the suitable commercially available conductive adhesives. Fuel supply has been given through the middle piece. Figure 1 explains the schematic design. Cutting molds were designed for cutting the sheets into desired size with textures on them creating gas flow channels (GFCs). They contribute in reduction of machining cost and manufacturing time for mass production purposes. Mechanical strength (flexural strength) values, contact resistance and through-plane electrical conductivity were obtained with the final three-layer bipolar plate. Following are some of the technical targets for PEM bipolar plates as defined by DOE for the year 2020 [5].

1. Cost (3 $ / kW)
2. Electrical Conductivity ($>$ 100 S/cm)
3. Flexural Strength ($>$ 25 MPa)
4. Aerial Specific Resistance (0.01 $\Omega.cm^2$)

4.2 Experimental

4.2.1 Materials

Expanded graphite-polymer composite (SIGRACET- TF6) sheets of 0.6 mm thickness were used for preparing the bipolar plates. These plates will be mentioned as EG sheets through the manuscript for easy understanding. A commercially available adhesive (AA-DUCT 902 Silver Epoxy Adhesive) is used for gluing EG sheets. The adhesive used has

excellent electro-mechanical and chemical properties especially electrical resistivity as low as 0.0001 Ω.cm. Commercially available Nafion XL membrane was used for our fuel cell performance testing. Custom made MEA was prepared with Pt loading of $0.46 mg.cm^{-2}$ and $0.47 mg.cm^{-2}$ for anode and cathode respectively. Commercially available Nafion XL membrane was selected and Tanaka catalyst with a composition of (38% wt Pt/C) was used for preparing MEAs. Decal transfer process was used to transfer catalyst on membrane by screen printer. Gasket thickness was calculated based on the thicknesses of membrane and GDL. Silicon Gasket with a thickness of 0.125 mm was used. Aluminum end plates were used for providing sufficient contact between the components. Copper plates with a thickness of 0.8 mm were used as current collector electrodes.

4.2.2 Bipolar plate and reactants flow filed design

Many types of fuel flow fields have been reported in literature. For our application a double serpentine flow field design was selected for anode side and straight channels for cathode side. EG sheets were used for preparing the bipolar plates. The idea was to cut anode and cathode channels on separate sheets and then joining them together with a third sheet in the middle to isolate the gasses. A schematic exploded view of three-layer bipolar plate is shown in Figure 4.1. While schematic showing anode and cathode side channel design is shown in Figure 4.2 and 4.3.

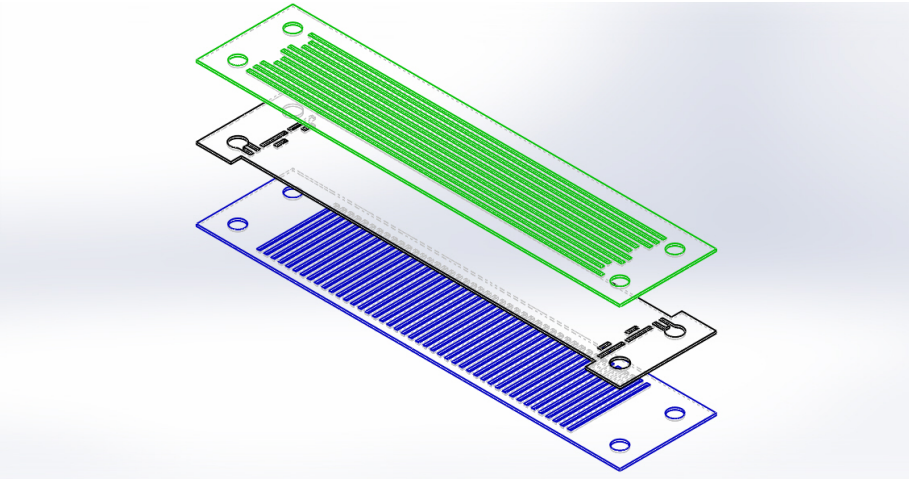

FIGURE 4.1: Three-layer bipolar plate model

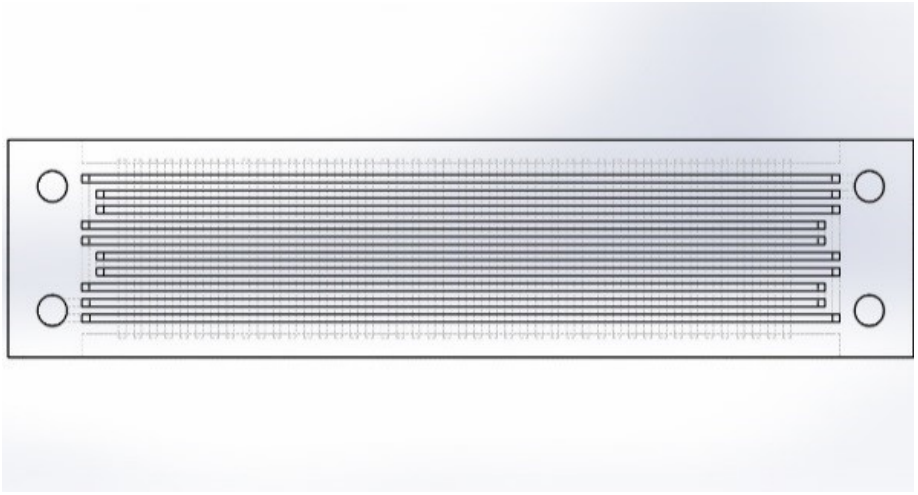

FIGURE 4.2: Bipolar plate - Anode side up

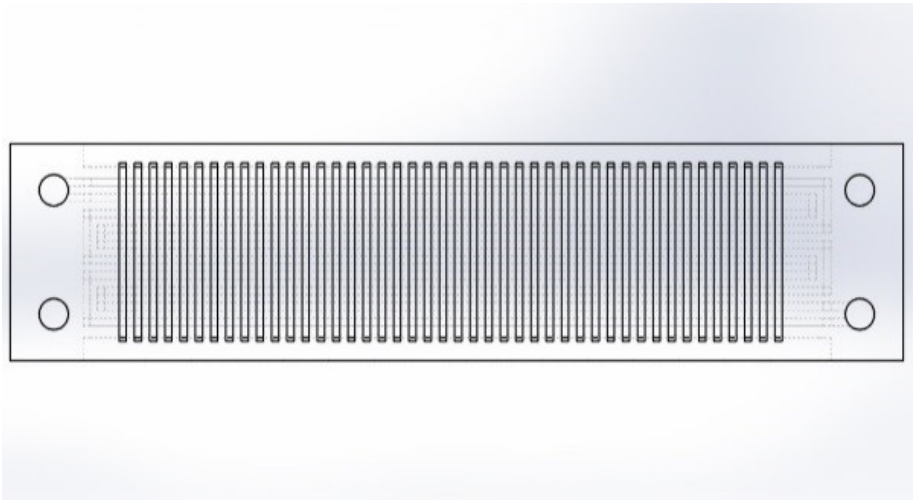

FIGURE 4.3: Bipolar plate - Cathode side up

4.2.3 Design of cutting Molds

Three different cutting molds were designed for cutting flow field channels on anode, cathode and middle plate sides respectively. Each mold consists of three parts;

1. Male part having sharp cutting blades of desired channels dimensions.
2. Female part having grooves of desired channel dimensions.
3. A stopper PTFE plate for supporting the female part and preventing the blades from further moving.

The idea is to hold the thin EG sheet between female and stopper plates and cut the channels by male part using hydraulic press. The blades of the male piece was selected as

double blades to avoid bending of the sheet to the channel. The grooves on female part guide the blades to cut the channels with desired dimension whereas land area support the EG sheet edges while cutting. The stopper plate is a hard PTFE material which can withstand the hydraulic press pressure without damaging the cutting blades. The blades on male part are placed apart according to the desired dimensions. A simple schematic of mold (cathode side) is shown in Figure 4.4.

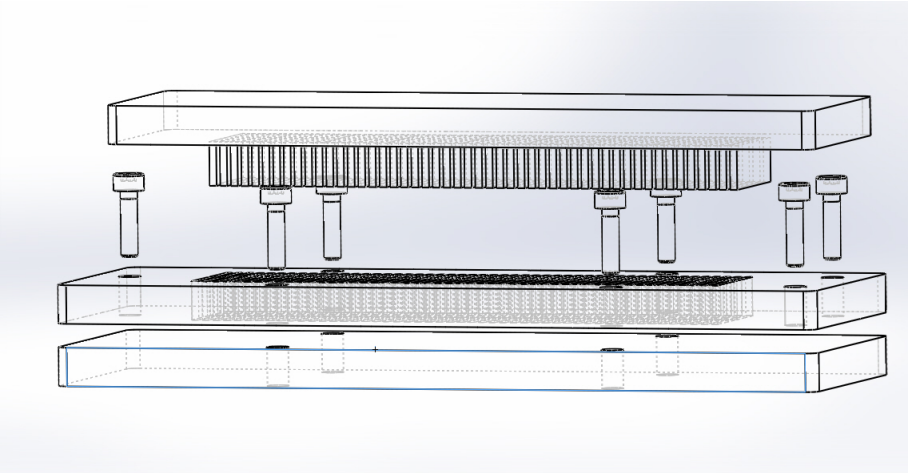

FIGURE 4.4: Mold Assembly (Cathode side)

The whole process consists of following steps:

1. Clamping the sheet between females and stopper plates using fasteners.
2. Aligning the male part with grooves.
3. Pressing the male part with an appropriate pressure using hydraulic press.
4. Un-clamping the mold and part inspection.

The crucial point here is to provide appropriate support to the edges of the sheet while cutting to avoid cracking and displacement of material inside for cutting channels with varying dimensions. Some of the material will be displaced while cutting and will increase the concentration on the edges. The portion which will cut goes inside the space between the cutting blades with the support of the stopper plates. The blade edges will rest on the stopper plate after cutting. The male part have to be cleaned from trapped material before making the next cut.

4.2.4 Preparation of Bipolar Plates

EG-polymer composite sheets were cut into desired size. Three-piece cutting molds were designed each for Anode, cathode and middle plates. The molds can cut the sheets into size and create gas flow channels in a single press punch. The whole process consists of the following steps:

1. EG sheet was clamped inside the two female mold pieces and male part was pressed creating flow channels.
2. Electrically conductive adhesive was applied on anode and cathode pieces using a semi-automatic screen printer (ATMA AT-45PA) to get uniform layer.
3. The three pieces were gently pressed together for proper adhesion.
4. Finally, this assembly was cured at $100°C$ for 15 minutes using BINDER FD 53 forced convection oven (shown in Figure 4.5). Finished parts were cleaned before placing them into single cell assembly.

Prototype of three separate layers of bipolar plate is shown in Figure 4.6.

FIGURE 4.5: Forced convection oven

FIGURE 4.6: Three layer bipolar plate prototype

4.2.5 Characterization of the bipolar plate

The 3-layer finished polymer composite bipolar plates were tested to obtain targeted mechanical (Flexural) strength, electrical conductivity and contact resistance properties. Several specimens prepared and tested to ensure repeat-ability. Standard characterization procedures were followed as applied by other researchers like Cho et al. and Landis et al. [19, 58].

4.2.6 Mechanical Strength Measurements

Several tests and techniques have been followed for determining the mechanical strengths of bipolar plates. These include tensile strength test method, compression test method and three point bending method. Three-point bending method was selected for our

measurements since this method represents the tensile and compression stresses occurring simultaneously at bipolar plates during assembly or compression of PEM fuel cell stacks. [16, 36, 39, 59, 60]. 3-point Instron Model 5569 universal testing machine was used to measure Flexural strength of the 3-layer bipolar plates. ASTM D790 standard was followed for making mechanical measurements. $16x60mm^2$ sized specimens were prepared and tested for Flexural strength. 3-point span distance was used to be 40 mm and moving with a constant cross head speed of 1 mm/sec.

4.2.7 Contact Resistance

In a typical PEM fuel cell stack, the contact resistance between bipolar plate and MEA layers have a great effect on cell performance than bulk resistance of those layers. Standard procedures were followed to measure contact resistance between BPP and GDL. Various authors in literature have applied the same methods to measuring contact resistance, references [61, 62] are relevant. The 3-layered Expanded Graphite composite samples with a thickness of 1.8 mm were placed between two carbon papers. and, the sandwiched between Gold coated metal plate at the ends. Current was passed through Gold coated plates and voltage drop between these plates was measured. Gradually, the compression pressure was increased step by step and measurements were recorded to see the effect of compression pressure. Contact resistance calculations were made according to Ohm's law.

4.2.8 Electrical Conductivity Measurements

Six samples were prepared to measure electrical conductivity. Standard procedure was followed as reported by Du et al., [32]. For obtaining in plane electrical conductivity, Jandel RM3-AR instrument was used for measuring electrical conductivity by 4-point probe measuring method. While for through plane electrical conductivity, custom made electrode plates were used for making measurements. An adjustable hydraulic press was used along with a Keithley Model 2000, 6 $\frac{1}{2}$ digit digital multi-meter. Electrical conductivity values were made by applying $140N.cm^{-2}$ pressure at the same time and all 4-probes were recorded for all specimens.

4.2.9 Weight Measurements

Weight of the finished bipolar plates was recorded using a precise (5 digit) weighing balance (Denver Instrument Germany TB-215D). Weight density and weight per kW calculations were made for the sake of DOE targets and comparison with studies done previously.

4.3 Results and Discussion

4.3.1 Physical and Mechanical Properties

The custom made three-layer bipolar plate had a density of $1.79 g/cm^3$. Different specimens were prepared for different measurements. Mechanical properties were obtained with 60 mm x 16 mm specimens. Five samples each 1.2 mm thick were tested for flexural strength and the values between 25 - 29 MPa were obtained. Results of one of the samples are depicted in Figure 4.7. These results satisfy the DOE targets and are excellent in terms of strength for PEM fuel cell bipolar plates manufacturing.

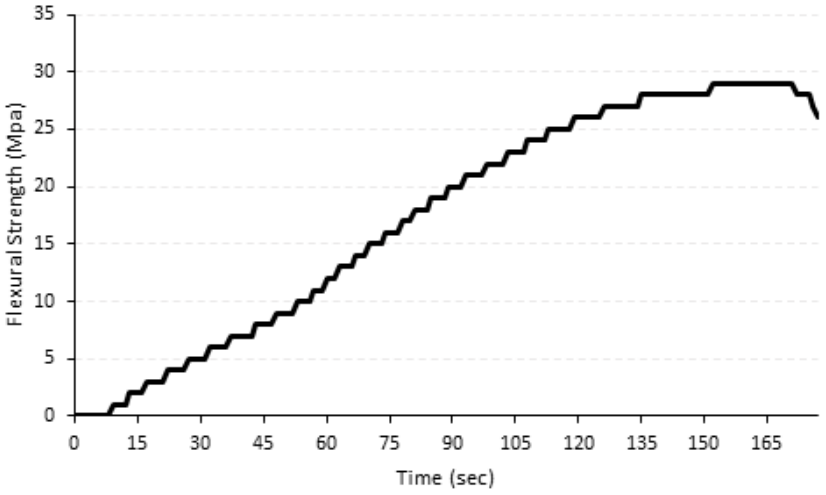

FIGURE 4.7: Flexural strength

4.3.2 Electrical Properties

Electrical conductivity measurements were conducted under $140N.cm^{-2}$ (14 bars) pressure. Three-layer EG composite samples were tested under various compression pressures to observe the effect of pressure. Aerial resistance average values of $22.3m\Omega.cm^2$ was achieved at $140N.cm^{-2}$ compression pressure. Aerial resistance measured at various compaction pressure is illustrated in Figure 4.8. DOE 2017 target for aerial resistance is $20m\Omega.cm^2$. Our results are in close approximation to the desired values.

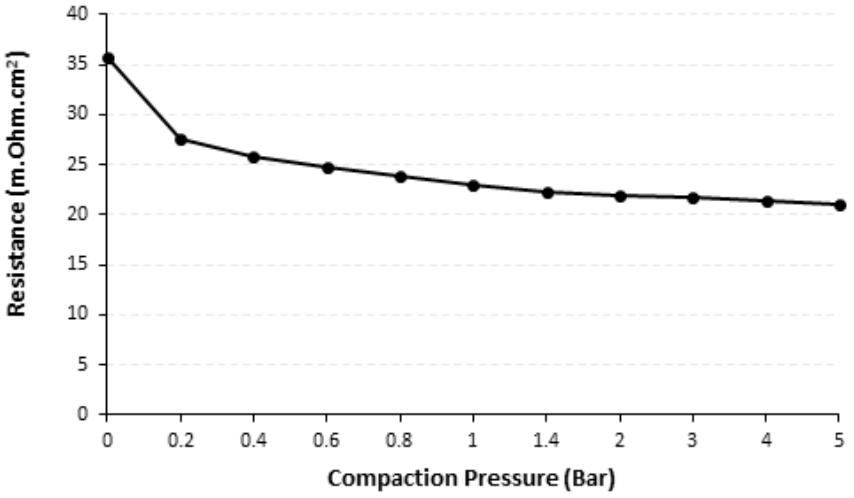

FIGURE 4.8: Aerial Resistance of three-layer EG composite at various compaction pressures

4.3.3 Cost and Weight Analysis

Average weight of the three-layer bipolar plate was measured to be 11.139 g, giving a value of 0.55 kg /kW (This value is calculated for stack assemblies) which is slightly higher than the DOE targets. The DOE target of 0.4 kg/kW can easily be achieved if higher power densities were achieved with better MEAs and optimized operating parameters. Thus, the bipolar plates prepared using this approach are strong candidate for light weight PEM fuel cell applications. Three-layer EG composite bipolar plate manufacturing cost analysis was made similar with other researchers. [63–65]. Cost elements which were added to calculate the total fabrication cost as shown in Figure 4.9. Material cost, tooling cost, labor cost, energy cost and other miscellaneous costs were all taken into account to obtain the manufacturing cost. When all parameters were taken into account the total manufacturing cost was calculated to be 7.77 \$/kW. Among others the material cost (EG

composite sheets and adhesive) is on top with a share of 46 %. This cost seems to be far away from DOE targets, however, this analysis is sensitive to various contributing factors that can be controlled. First of all, material cost can be reduced for mass production. Secondly, labor cost which is totally dependent on hands on process time, can be reduced if we go for a complete automated process. However, this will slightly increase the initial capital cost. Finally, better performing MEAs enable smaller plates which will decrease the material cost furthermore. The total cost can drop down to DOE target of 3 $/kW if whole production is initialized with indicated improvements.

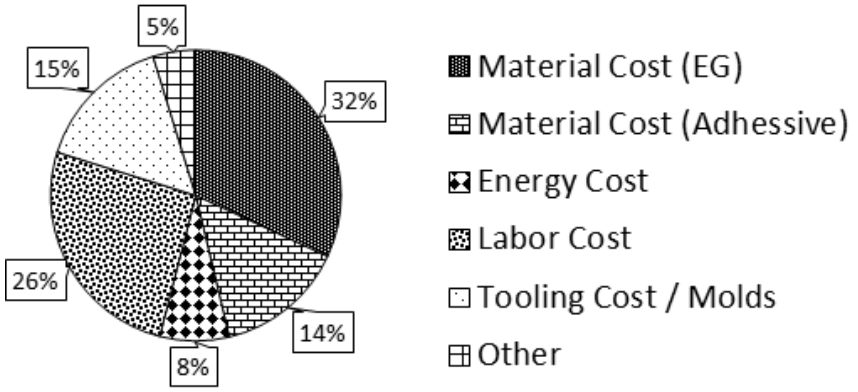

FIGURE 4.9: Cost elements for manufacturing three-layer EG composite bipolar plate

4.3.4 Fuel Cell performance

3-layer bipolar plates prepared were tested for performance in actual test environment. Custom built Fuel cell test station at our labs was used for performance tests (shown in Figure 3.13. The tests were performed at $55°C$ and the reactant gases were humidified at $50°C$. Reactant gas flow rates were maintained constant (as $0.2l.min^{-1}$ and $0.4l.min^{-1}$) both for the anode and cathode respectively. The MEAs were conditioned before recording experimental results. Polarization and power values were taken after six continuous cycles. Polarization and power best describe the output of a fuel cell. The results obtained are shown in the following graphs The results obtained are shown in Figure 4.10 below.

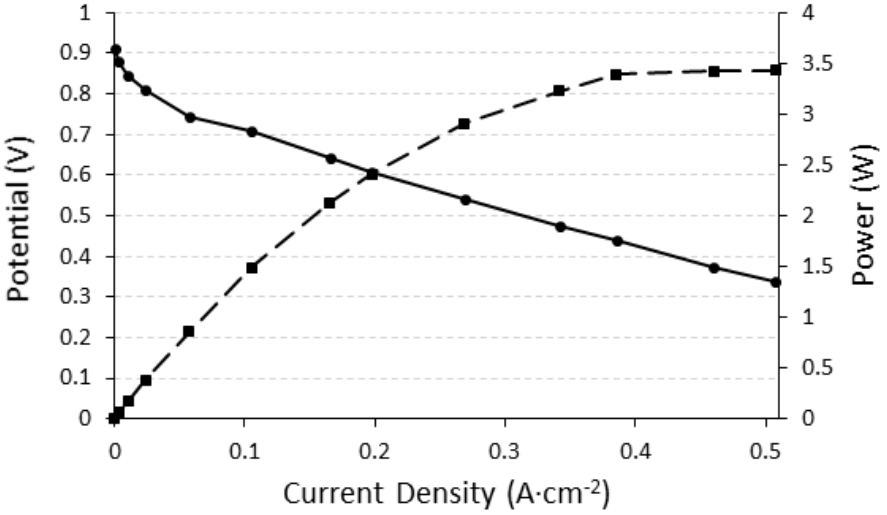

FIGURE 4.10: Fuel Cell performance - Polarization and Power curves

4.4 Main Crux / Remarks

Main focus, in this study, was to prepare light weight and low cost bipolar plates by an alternate fabrication method. Purpose was to float an idea about this cost effective and easy to manufacture technique for bipolar plate production at lab scale. Efforts were put together to prepare three-layer expanded graphite-polymer composite bipolar plates using conductive epoxy adhesive. Low cost cutting molds were designed and fabricated for creating reactant gas flow fields. The final product was evaluated in terms of its weight, cost and performance for PEM fuel cells. With this novel technique we have been able to achieve the desired mechanical strength and areal specific resistance. These results are very encouraging for the production of PEM fuel cell bipolar plates using this technique. Although cost and weight do not meet DOE targets, however, they can be reduced significantly by getting whole scale production prices on material cost, reducing the production cycle time by process automation, getting higher current and power densities using efficient MEAs, and operating parameters optimization. The final product in superior for light weight, low cost and high performance applications.

Chapter 5

Experimental determination of optimal clamping torque for AB-PEM Fuel cell

5.1 Introduction

PEM fuel cell performance is significantly effected by stack design and cell assembly. The importance of this chapter will be clear from subsequent paragraphs which cover references from the literature. Optimum contact pressure is necessary between the components to hold them together in the fuel cell stack. The contact pressure ensures leakage prevention of the reactant gases between the layers and minimize the contact resistance between layers. The fuel cell stack clamping force is the sum of force required to compress the gasket, fuel cell layers, and internal force. Fuel cell stack comprises of diverse characteristics components. Bipolar plates and end plates are hard enough to withstand high compression or elongation forces while MEAs, GDL and gasket are very thin and may be damaged with excessive loading. On the other hand the contact between the components may lose if less force is applied to make them unite. An adequate uniform assembly force must be determined for getting an optimal point that ensures good mechanical contact as well prevent over compression of individual components. If we examine the issue in more detail, in-adequate and non uniform pressure will result leakage of reactant gases and increasing the contact resistance between the cell components

which will consequently reduce cell performance and cause degradation issues. While over compression of the components can cause mechanical damage to the components and also GDL over compression can cause mass transport hindrance again resulting in cell performance loss and degradation issues. So, the crux of all this discussion is that an optimum assembly force is always there and need to be determined. This force also depend upon the fuel cell component materials and and stack design. Several studies have been carried out to determine optimal clamping force in order to achieve optimal fuel cell performance. Alex et al performed Simulation of a single cell and 16-cell Fuel Cell at various clamping pressures. They performed experimental procedures for observing clamping pressure effects on a 16-cell stack. They placed a thin pressure-sensitive film between GDL and bipolar plate and applied clamping pressure using various loads and duration. They used two types of GDLs and obtained detailed 3D plots of stress and deformation [66]. Chang et.al worked on GDL porosity, gas permeability and electrical resistance properties using a special designed test system. Further, they also performed experiments to measure contact resistance between the GDL and BPP at a range of clamping pressures. They concluded that an increase in clamping pressure decreases the inter-facial resistance between BPP and GDL. This results in gain of electro-chemical performance. On the contrary, at high clamping pressure values, increase in clamping pressure reduces the Ohmic resistance as well as narrows down the diffusion path for mass transfer from gas flow fields to the electrode layer [67]. Woo Kum et al. [68] reported varying PEM fuel cell performance with compression pressure resulting from torque applied on bolts. The researchers utilized three different types of GDLs and concluded that the optimum is related to the gasket thickness. Further, they measured compression pressure on the GDLs. Wang et al studied the effects of internal pressure distribution on the performance of a PEM fuel cell stack. They designed a pressurized end plate and used pressure sensitive films to measure the pressure distribution for both conventional and newly designed end plates and recorded increase in cell performance with newly designed end plate [13].

Zhou et al studied clamping force effects on the cell performance with inter-digitated gas distributors. They take into account the contact resistance between the interfaces, GDL porosity distribution agd its deformation effects. They reported that an optimal clamping force is there at which the highest Power density can be achieved using inter-digitated gas distributors [69]. Shuo et al., performed Finite Element Analysis (FEA)

procedures to establish a PEM single cell stack with point stack assembly method [70]. Yu et al., designed a new asymmetric composite sand-wich end plate made of carbon fiber reinforced composite and glass fiber reinforced composite with a pre-curvature generated by the residual thermal deformation. The product yields the required pressure distribution in the stack when the end plates are fastened by the clamping device [71]. Liu et al., comprehensively studied the technique based on FEA model and Monte Carlo simulations approach to determine the effect of dimensional error of the metallic BPP on the pressure distribution of gas diffusion layer (GDL) [72]. Lin et al., reported the effect of gas diffusion layer compression on the performance in a PEM type fuel cell [73].

Zhou et al., worked on the effects of non-uniformity of the pressure distribution in reference to contact resistance. Acoording to their findings, the minimum electrical contact resistance is resulted by applying uniform pressure distribution [74]. Avasarala et al., studied Effects of surface roughness of composite bipolar plates on the contact resistance of a PEM fuel cell. They reported that the contact resistance is controlled by electrical properties of the interface-layer between the contacting surfaces [75]. Yung Wen et al., performed an experimental study of clamping pressure effects on the performance of a single PEM fuel cell and a 10-cell stack. They found that the uniform contact pressure distribution, the ohmic-resistance and the mass transport control current and have highly linear correlation with the mean contact pressure [76]. Montanini et al., measured the clamping pressure distribution in polymer electrolyte fuel cells using piezo-resistive sensor arrays and digital image correlation techniques and reported the pressure distribution effects [77]. Xing et al., presented a 3-D model to show the effect of assembly clamping pressure on the GDL properties. They determined that the performance of PEM fuel cells and optimum clamping pressures are related to each other. They used different operating voltage ranges and suggested that the optimum clamping pressures increase when the operating voltage increases [78].

5.1.1 Clamping Torque calculation Theory

Clamping torque on the bolts can be calculated from the following equation as explained by Barbir et al. [6]:

$$T_t = F_{clamp}.K_b.D_b/N_b \tag{5.1}$$

$$F_{clamp} = P_c.A \tag{5.2}$$

Where, T_t is the tightening torque in Newton meters (N.m), F_{clamp} is the clamping force in Newton (N), K_b is the friction coefficient, D_b is the bolt nominal diameter in meters (m), and N_b is the number of bolts. F_{clamp} is a function of clamping pressure (P_c) and cell active area (A). Colleen et al [3] also considered other important dimensions for calculating clamping torque i.e. Material properties of cell components and bolts, Geometry of holes, Stiffness of the components, Stack thickness, Contact resistance between BPP and GDL etc. The torque value obtained by these calculations give us range of clamping torque to be applied, but still there is need to find optimum torque value which will give optimum cell performance. A clamping torque value of 1.2 Nm was calculated for our fuel cell stack. This study focuses experimental procedure for obtaining optimum clamping torque. The effects of clamping force can be summarized in the following Figure 5.1.

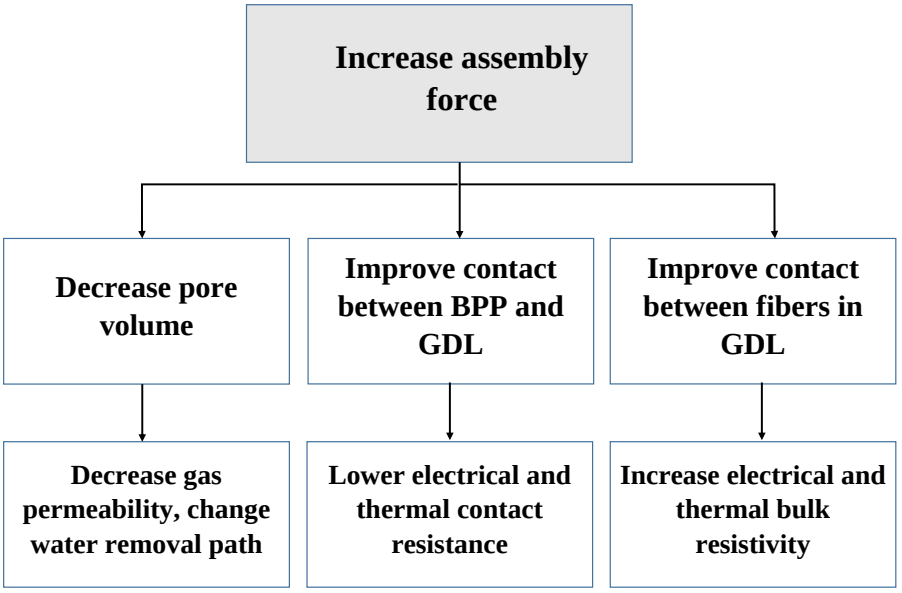

FIGURE 5.1: Effects of increasing assembly pressure

5.1.2 Contact Resistance and clamping Pressure

Contact resistance between GDL and BPP is caused by mating of two surfaces and depend on the surface topology of connecting faces. The contact resistance can be obtained as measured by various authors in literature [61, 62]. The governing equation

for calculations is given below;

$$R_{contact} = Res_1 - Res_2 - R_{BPP} - R_{GDL}/2 \tag{5.3}$$

Where, Res_1 and Res_2 are measured resistances from Setup 1 and Setup 2, respectively as shown in the Figure 5.2 and 5.3. R_{BPP} is the bulk resistance of graphite BPP and R_{GDL} is the bulk resistance of GDL. R_{BPP} and R_{GDL} are calculated according to their bulk resistivity. Contact resistance was observed to be minimum at a value of $140 N/m^2$.

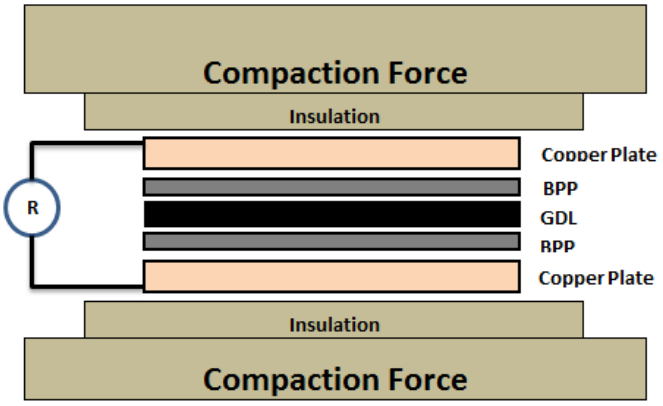

FIGURE 5.2: Contact Resistance measurement-configuration 1)

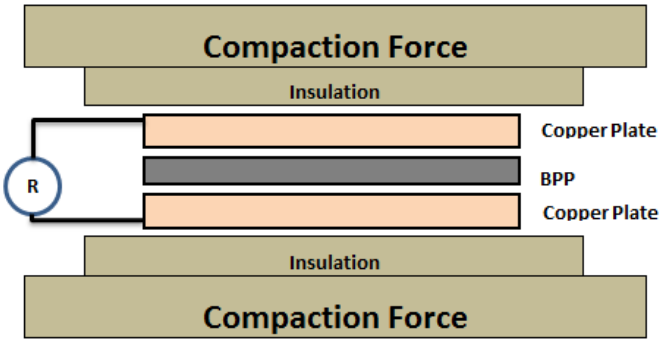

FIGURE 5.3: Contact Resistance measurement-configuration 2

5.2 Experimental

5.2.1 Materials, Method and Assembly

Graphite bipolar plates with double serpentine flow channels for anode and straight through flow channels for cathode side were prepared by machining. Commercially

available Nafion 212 membrane was selected for our fuel cell. Custom made MEAs were prepared with a Platinum (Pt) contents of $0.6 mgcm^{-2}$ for each anode and cathode sides. Gasket thickness was calculated based on the thicknesses of membrane and GDL. Silicon Gasket with a thickness of 0.125 mm was used. Polymer (PTFE) end plates were used for providing sufficient contact force between the components. A total quantity of 08 M4x20 bolts were used to clamp the cell components. Copper sheets with a thickness of 0.8 mm were used as current collector electrodes. Multiple MEAs were prepared and tested to make sure repeat-ability. MEAs were prepared with an active area of 10 cm x 2 cm. Other components were also prepared as per designed dimensions with acceptable properties as defined by Department of Energy (DOE). Finally, a single cell was assembled for testing at different clamping torque values.

5.2.2 Contact Resistance Measurement

Standard contact resistance measurement setups have been followed by several authors like Mishra et al., and Zhang et al. [61, 62]. I used the similar procedures to measure the contact resistance. BPP specimen was inserted between two carbon papers (GDL) and all sand-witched between copper current collectors. We have developed a customized setup for contact resistance measurement at our labs. The system is capable of applying a range of compression pressure. Experiments were performed to measure contact resistance at various compression pressures with an increment of 0.5 MPa. Measurements were repeated five time times to obtain reliable and repeatable results.

5.2.3 Pressure Distribution

Pressure distribution measurement method as used by several authors [70, 76, 79] has been followed for our experiment. To get the pressure distribution, tests were conducted on our hardware with 8 bolts at five different applied torques from 0.5 to 2.5 Nm with an increment of 0.5 N.m. A rectangular piece of film was cut with the dimension similar to BPP used and was inserted between the membrane electrode assembly (MEA) and gas diffusion layer (GDL). Firstly 0.5 N.m torque was applied on each 8 bolts of the cell structure in a certain sequence. After approximately 5 min, the bolts were loosened and the film was taken out. Same procedure was repeated with other torque values and pressure distribution was observed.

5.3 Results and Discussion

5.3.1 Pressure distribution results

With the application of pressure, the micro-capsules on the pressure sensitive film (a pair of films) placed between BPP and MEA broke up producing red color material. The color released by one film was absorbed on the other film producing the BPP face impression on it. The intensity of the color represent a direct correlation with the applied pressure. More the pressure applied, more intense the red pattern and vice versa. The films were removed from the assembly five minutes after the pressure applied. It has been observed that pressure distribution was uniform at a clamping torque of 1.5 N.m compared to other torque values. Figures **??** and **??** below show the experimental results obtained at 0.5 N.m and 1.5 N.m torque values respectively.

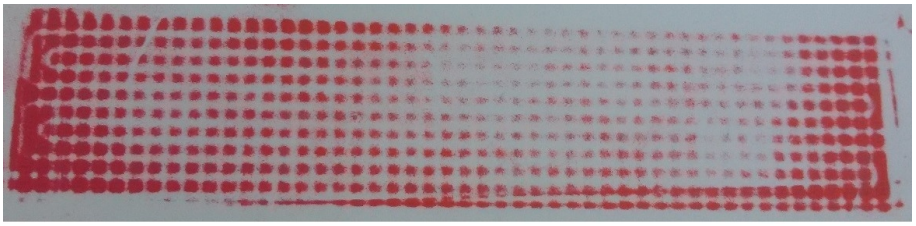

FIGURE 5.4: Pressure distribution - Torque applied 0.5 N.m

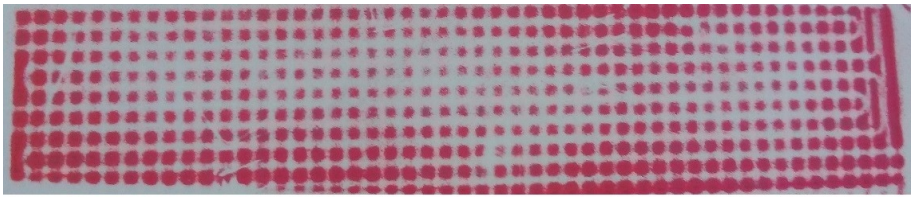

FIGURE 5.5: Pressure distribution - Torque applied 1.5 N.m

5.3.2 Single Cell Performance

Assemblies were prepared by applying different torque values step by step and performance measured. Custom built Fuel cell test station at our labs was used for performance tests (shown in Figure 3.13. The tests were performed at $55°C$ and the reactant gases were humidified at $50°C$. Reactant gas flow rates were maintained constant (as $0.2l.min^{-1}$ and $0.4l.min^{-1}$) both for the anode and cathode respectively. The MEAs were conditioned before recording experimental results. Polarization and power values were taken after six continuous cycles. Polarization and power best describe the output

of a fuel cell. PEM fuel cell performance was obtained experimentally as shown in Figure 5.6 and 5.7. The fuel cell performance results clearly follow the theoretical calculations made. The fuel cell performance was observed to be low at small applied torque values and improves with the increase of applied torque. Then, there is a value where it is observed to be the best. It starts lowering as we keep on increasing torque value. Hence, the optimum is the torque value at which best performance was obtained. The reason can be explained as discussed in above sections. For a lower value of assembly torque (0.5 N.m in this case), the compression pressure is not sufficient to compress GDL to gasket level and may cause fuel leakage as well as a poor contact between GDL and bipolar plate. On the other hand, higher assembly torque (2.5 N.m) leads to smaller porosity, which imposes more impedance to gas transfer, lowering cell performance. The optimum clamping torque (1.5 N.m) is a negotiation between contact resistance and mass transfer due to GDL compression giving the best cell performance.

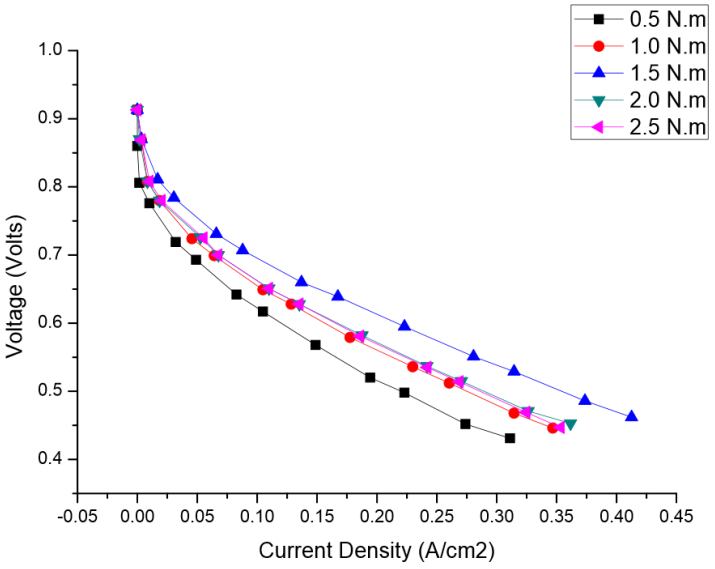

FIGURE 5.6: Polarization at different clamping torque values

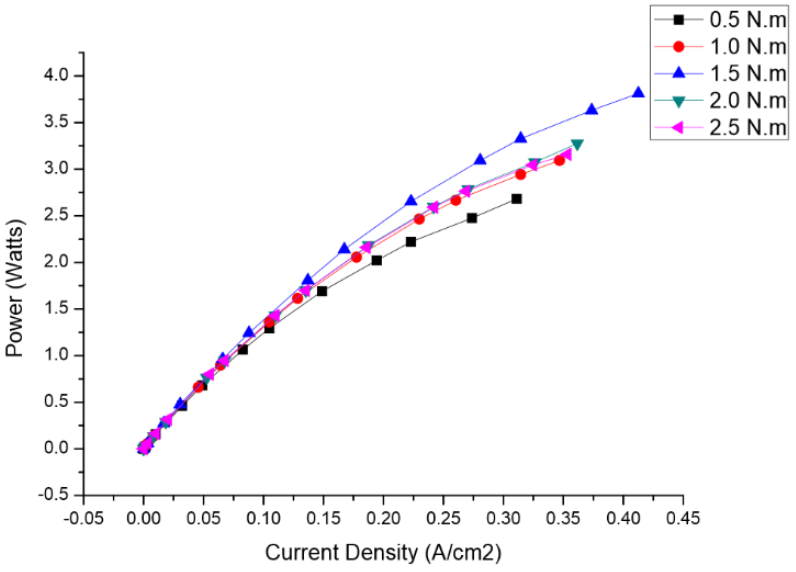

FIGURE 5.7: Power at different clamping torque values

5.4 Summary of the study

In order to study the effects of assembly pressure on the performance of PEM fuel Cells, theoretical calculations were made for calculating the clamping torque value. Experimental procedures were carried out for obtaining the optimized clamping torque giving optimal performance. Fuel cell performance has been observed by polarization and power curves. It has been observed that assembly pressure has noteworthy effects on PEM fuel cell performance. In a broader view, low assembly pressure causes fuel leakage problems and an increase in contact resistance between bipolar plates and GDL, consequently decreasing fuel cell performance. Whereas, larger assembly clamping pressure increases mass transfer resistance and hence lowering cell performance. Therefore, the crux of this study is clear that there exist an optimum clamping pressure for each fuel cell stack which offers best performance.

Chapter 6

Conclusion and Future Work

6.1 Summary and Conclusion

Polymer exchange membrane fuel cells (PEMFC) are the devices that directly convert Chemical energy into Electrical energy and are potential candidates for portable and stationary power supply applications due to their several advantages over combustion engines. Among several challenges, cost and weight of PEMFC are prominent factors to be controlled for its commercialization. PEMFC bipolar plates are the components that share the major weight and cost of the overall fuel cell stack. This study has been carried out to develop PEMFC stack for small Unmanned Aerial Vehicle (UAV) application with a power requirement of 200W. Air breathing and air cooling PEM Fuel cell system was designed using graphite material for bipolar plates.

The research on manufacturing processes and performance modeling / simulations of PEM fuel cells links with the fast growing fuel cell technology and demands of high production volumes. While we go for mass productions, the understanding of fabrication techniques and assembly processes become essentially critical. Because, fabrication and assembly methods are directly linked with the performance and durability. This study is more focused on electro-mechanical properties of fuel cell components. This thesis covers the basic understanding of electro-chemical reactions and performance of PEM fuel cell as well new approach to manufacture one of the most important components of fuel cell i.e. bipolar plates. Also, assembly procedures have been studied in detail in the context of optimizing fuel cell performance.

Following paragraphs provide a more comprehensive summary and concluding remarks of this study. Firstly, an effort was put to fabricate light weight, cost effective and reliable bipolar plates. It is emphasized to utilize the simulated results for achieving optimal experimental results. Keeping in view the available space and weight constraints of UAV, I have optimally designed the shape of active area (10 cm x 2 cm) and flow channels. Fluid flow analysis using ANSYS Fluent software was performed on different channel shapes and an optimal design (double serpentine), with least pressure drop and optimal velocity profiles, was selected. Electro-chemical simulations were also done to predict the fuel cell performance (IV and Power curves) using MATLAB software prior manufacturing the prototype. Moreover, for the sake of DOE targets, initial tests were performed on single cell. Encouraging results of Current and Power densities were achieved, close to the designed parameters. Secondly, bipolar plates were more focused in terms of alternate efficient material, novel design and fabrication process. A number of graphite polymer composites have been reported in literature with excellent electro-mechanical properties and chemical stability. Compression molding and Injection molding are the most common manufacturing methods being used for mass production. In this section, an alternate fabrication technique was studied comprehensively in an attempt to develop low cost and light weight Expanded Graphite (EG) polymer composite bipolar plates for air breathing PEM fuel cell. Cutting molds were designed to cut channels on thin (0.6 mm) commercially acquired EG sheets. Three separate sheets, with flow channel textures removed, were glued to each other by a commercial conductive epoxy to build a single bipolar plate. The final product had a density of $1.79 g/cm^3$. A bipolar plate with a $20 cm^2$ active area weighed only 11.38 g. Manufacturing cost was estimated to be 7.77 $ / kWe and total manufacturing time of 2 minutes / plate was achieved with lab scale manufacturing. Flexural strength value of 29 M.Pa was obtained with three-point bending experiment. Total resistance of $22.3 m\Omega.cm^2$ was measured for the three layer bipolar plate. Fabrication process devised can be good alternate for small scale as well as mass production. Thirdly, an important issue of fuel cell assembly, performance optimization and degradation was studied. PEM fuel cell stack is provided with an appropriate clamping torque to prevent leakage of reactant gases and to minimize the contact resistance between gas diffusion media (GDL) and bipolar plates. GDL porous structure and gas permeability is directly affected by the compaction pressure which consequently drastically change the fuel cell performance. Various efforts have been made to determine

the optimal compaction pressure and pressure distributions through simulations and experimentation. Lower compaction pressure results in increase of contact resistance and also chances of leakage. On the other hand, higher compaction pressure decreases the contact resistance but also narrows down the diffusion path for mass transfer from gas channels to the catalyst layers consequently lowering cell performance. The optimal cell performance is also associated with seal thickness and assembly compression pressure acting on GDL. Each fuel cell stack require a unique optimal assembly pressure due to differences in its fuel cell component materials and stack design. In this section, compaction pressure at minimum contact resistance was determined and clamping torque value was calculated accordingly. Single cell performance tests were performed at five different clamping torque values (0.5 N.m, 1.0 N.m, 1.5 N.m, 2.0 N.m & 2.5 N.m) for achieving optimal cell performance. Experimental and theoretical results were compared for making inferences about optimal cell performance. A clamping torque value of 1.5 N.m was determined experimentally to be the best for getting optimal performance for this specific fuel cell. The major achievements and original contributions of this research can be summarized in three parts;

1. A problem based study was carried out to best select the shape of bipolar plate channels through simulations in order to achieve optimum cell performance. Also, electro-chemical simulation was done to predict fuel cell performance prior manufacturing. It has been observed that Double serpentine is the best design option for this type of fuel cell active area based on design criteria.

2. A novel bipolar plate was designed with new material and alternate fabrication technique and prototype manufactured. The final product was characterized to see desired properties and compared with the target values. The final bipolar plate obtained was light weight and low cost superior product for various small vehicle applications.

3. Fuel cell stack assembly procedures and clamping pressure affect cell performance significantly. Experimental study was performed to find out optimum clamping Torque and hence force which consequently exhibited optimum performance. It can be concluded that for every cell there exist an optical clamping torque at which maximum performance can be obtained.

6.2 Future Work

The simulations and experiments performed in this research can be further improved and /or extended in the following directions:

1. To predict membrane dry out and flooding conditions and factors, water and heat management in fuel cell can be simulated using ANSYS Fuel cell module for better understanding and control of heat and water management.

2. BPPs production technique proposed here can be further improved by designing new type of cutting molds. One novel idea can be to cut flow channels on EG sheets is by wire cutting molds. Wire molds can engrave flow channels with any pattern and can generate bend at any desired radius. This can be a very low cost solution for mass production of BPPs.

3. Balance of plant (BOP) are the necessary components for controlling temperature, humidity, fuel flow rates and pressure of reactant gases. There is need to work on BOP for optimizing fuel cell performance.

4. Fuel cell stack sealing is very important for leakage prevention and performance degradation. New sealing materials and methods need to be devised for improving performance and durability.

5. Fuel cell degradation, reliability and durability issues are of utmost importance and must be worked out. Degradation rates and life determination through various algorithms, simulations and experiments can be studied in more details to help commercialize the fuel cells.

6. Optimization methods need to be developed for assembly processes under various operating conditions and for component design.

Bibliography

[1] D. Papageorgopoulos. Doe fuel cell technology program overview and introduction to the 2010 fuel cell pre-solicitation workshop in doe fuel cell pre-solicitation workshop, 2010. Department of Energy, Lakewood, Colorado.

[2] G. Wand. Fuel cell history. Part One. 14.

[3] Colleen and Spiegel. *PEM Fuel cell modelling and simulation using MATLAB*. Elsevier, 2008.

[4] Qun, Hongyun, and Kang. An improved tlbo with elite strategy for parameters identification of pem fuel cell and solar cell models. *International journal of hydrogen energy*, 39:3837–3854, 2014.

[5] Fct fuel cells types of fuel cells, 2009. [Online]: http://www1.eere.energy.gov/hydrogenandfuelcells/fuelcells/fc-types.

[6] Barbir and Frano. *PEM Fuel Cells: Theory and Practice*. Elsevier Academic Press., 2005.

[7] E. Hontanon. Optimisation of flow field in pem fuel cell using cfd techniques. *Journal of Power Sources*, 86:363–368, 2000.

[8] A. Kumar, Reddy, and G. Ramana. Effect of channel dimensions and shape in the flow field distributor on the performance of pem fuel cells. *Journal of Power Sources*, 113:11–18, 2003.

[9] S. Gamburzev, C. Boyer, and A.J. Appleby, 1998.

[10] D.S. Watkins, K.W. Dircks, and D.G. Epp, 1992. US Patent No. 5,108,849.

[11] D.S. Watkins, K.W. Dircks, and D.G. Epp, 1991. US Patent No. 4,988,583.

[12] X. Li. Pem fuel cells., 2002. Lecture notes, University of Waterloo.

[13] Wang Xinting, Song Ying, and Zhang Bi. Experimental study on clamping pressure distribution in pem fuel cells. *Journal of Power Sources*, 179:305–309, 2008.

[14] F. Mighri, Huneault, and Champagne. Electrically conductive thermoplastic blends for injection and compression molding of bipolar plates in the fuel cell application. *Polymer Engineering and Science*, 44(9):1755–1765, 2004.

[15] B. Zhu. Study on the electrical and mechanical properties of polyvinylidene fluroide/titanium silicon carbide composite bipolar plates. *Journal of Power Sources*, 161(2):997–1001, 2006.

[16] O.L. Adrianowycz. Next generation bipolar plates for automotive pem fuel cells, 2009. Graftech International Ltd.

[17] A. Kumar and R.G. Reddy. Materials and design development for bipolar/end plates in fuel cells. *Journal of Power Sources*, 129(1):62–67, 2004.

[18] J. Scholta. Development and performance of a 10 kw pemfc stack. *Journal of Power Sources*, 127(1-2):206–212, 2004.

[19] E.A. Cho. Characteristics of composite bipolar plates for polymer electrolyte membrane fuel cells. *Journal of Power Sources*, 125(2):178–182, 2004.

[20] E.A. Cho, H.L. Wang, and J.A. Turner. Ferritic stainless steels as bipolar plate material for polymer electrolyte membrane fuel cells. *Journal of Power Sources*, 128 (2):193–200, 2004.

[21] J.S. Cooper. Design analysis of pemfc bipolar plates considering stack manufacturing and environment impact. *Journal of Power Sources*, 129(2):152–169, 2004.

[22] K.M. El-Khatib. Corrosion stability of sus316l hvof sprayed coatings as lightweight bipolar plate materials in pem fuel cells. *Anti-Corrosion Methods and Materials*, 51 (2):136–142, 2004.

[23] E. Fleury. Fe-based amorphous alloys as bipolar plates for pem fuel cell. *Journal of Power Sources*, 159(1):34–37, 2006.

[24] Y. Wang and D.O. Northwood. An investigation into polypyrrole-coated 316l stainless steel as a bipolar plate material for pem fuel cells. *Journal of Power Sources*, 163(1):500–508, 2006.

[25] Y. Wang and D.O. Northwood. An investigation of the electrochemical properties of pvd tin-coated ss410 in simulated pem fuel cell environments. *International Journal of Hydrogen Energy*, 32(7):895–902, 2007.

[26] Y. Wang and D.O. Northwood. An investigation into tin-coated 316l stainless steel as a bipolar plate material for pem fuel cells. *Journal of Power Sources*, 165(1): 293–298, 2007.

[27] R.F. Silva. Surface conductivity and stability of metallic bipolar plate materials for polymer electrolyte fuel cells. *Electrochimica Acta*, 51(17):3592–3598, 2006.

[28] J. Huang, D.G. Baird, and J.E. McGrath. Development of fuel cell bipolar plates from graphite filled wet-lay thermoplastic composite materials. *Journal of Power Sources*, 150(0):110–119, 2005.

[29] H. Wolf and M. Willert-Porada. Electrically conductive lcpcarbon composite with low carbon content for bipolar plate application in polymer electrolyte membrane fuel cell. *Journal of Power Sources*, 153(1):41–46, 2006.

[30] T.J. Yen. A micro methanol fuel cell operating at near room temperature. *Applied Physics Letters*, 83:4050, 2003.

[31] Y. Wang. Fabrication and characterization of micro pem fuel cells using pyrolyzed carbon current collector plates. *Journal of Power Sources*, 195(15):4796–4803, 2010.

[32] L. Du and S.C. Jana. Highly conductive epoxy/graphite composites for bipolar plates in proton exchange membrane fuel cells. *Journal of Power Sources*, 172(2): 734–741, 2007.

[33] B. Dursun. Expanded graphiteepoxyflexible silica composite bipolar plates for pem fuel cells. *Fuel Cells*, 14(6):862–867, 2014.

[34] B. Unveroglu. Expanded graphite epoxy composites bipolar plates for pem fuel cells. *Ecs Transactions*, 41(1):1869–1877, 2011.

[35] L. Xu. Surface modification of a natural graphite/phenol formaldehyde composite plate with expanded graphite. *Journal of Power Sources*, 183(2):571–575, 2008.

[36] S.R. Dhakate. Expanded graphite-based electrically conductive composites as bipolar plate for pem fuel cell. *International Journal of Hydrogen Energy*, 33(23):7146–7152, 2008.

[37] L.N. Song. Short carbon fiber reinforced electrically conductive aromatic polydisulfide/expanded graphite nanocomposites. *Materials Chemistry and Physics*, 93(1): 122–128, 2005.

[38] C. Du. The preparation technique optimization of epoxy/compressed expanded graphite composite bipolar plates for proton exchange membrane fuel cells. *Journal of Power Sources*, 195(16):5312–5319, 2010.

[39] C. Du. Preparation and properties of thin epoxy/compressed expanded graphite composite bipolar plates for proton exchange membrane fuel cells. *Journal of Power Sources*, 195(3):794–800, 2010.

[40] R.K. Ahluwalia. Fuel cell systems analysis, 2009. Argonne National Laboratory. p. 919-924.

[41] Wang Y., S. Basu, and C.Y. Wang. Modeling two-phase flow in pem fuel cell channels. *Journal of Power Sources*, 179(2):603–617, 2008.

[42] X. Li and I. Sabir. Review of bipolar plates in pem fuel cells: flow-field designs. *Int. J Hydrogen Energy*, 30(4):359–371, 2005.

[43] F. Jiang. Simulation of a pemfc with zigzag flow field, 2010.

[44] D.H. Jeon. The effect of serpentine flow-field designs on pem fuel cell performance. *Int. J Hydrogen Energy*, 33(3):1052–1066, 2008.

[45] G. Inoue, Y. Matsukuma, and M. Minemoto. Effect of gas channel depth on current density distribution of polymer electrolyte fuel cell by numerical analysis including gas flow through gas diffusion layer. *J Power Sources*, 157(1):136–152, 2006.

[46] J.M. Correa, F.A. Farret, L.N. Canha, and M.G. Simoes. An electrochemical based fuel cell model suitable for electrical engineering automation approach. *IEEE Trans. on Industrial Electronics*, 51(5):1103–1112, 2004.

[47] J.C. Amphlett, R.M. Baumert, R.F. Mann, B.A. Peppley, and P.R. Roberge. Performance modeling of the ballard mark iv solid polymer electrolyte fuel cell. *J Electrochem Soc*, 142(1):1–15, 1995.

[48] J.M. Correa, F.A. Farret, L.N. Canha, and M.G. Simoes. Sensitivity analysis of the modeling parameters used in simulation of proton exchange membrane fuel cells. *IEEE T Energ Conver*, 20(1):211–2218, 2005.

[49] R.F. Mann, J.C. Amphlett, M.A.I. Hooper, H.M. Jensen, B.A. Peppley, and P.R. Roberge. Development and application of a generalized steady-state electrochemical model for a pem fuel cell. *J Power Sources*, 86(1):173–180, 2000.

[50] Z.J. Mo, X.J. Zhu, L.Y. Wei, and G.Y. Cao. Parameter optimization for a pemfc model with a hybrid genetic algorithm. *Int. J Energy Res*, 30(8):585–597, 2006.

[51] A. Hermann, T. Chaudhuri, and P. Spagnol. Bipolar plates for pem fuel cells: A review. *International Journal of Hydrogen Energy*, 30(12):1297–1302, 2005.

[52] Y.Z. Meng. Poly(arylene disulfide)/graphite nanosheets composites as bipolar plates for polymer electrolyte membrane fuel cells. *Journal of Power sources*, 160(1):165–174, 2006.

[53] R.H.J. Blunk. Enhanced conductivity of fuel cell plates through controlled fiber orientation. *AIChE Journal*, 49(1):18–29, 2003.

[54] C.K. Chen and J.K. Kuo. Nylon 6/cb polymeric conductive plastic bipolar plates for pem fuel cells. *Journal of Applied Polymer Science*, 101(5):3415–3421, 2006.

[55] L. Du. *Highly Conductive Epoxy/Graphite Polymer Composite Bipolar Plates In Proton Exchange Membrane (PEM) Fuel Cells.* Polymer Engineering, University of Akron: Ohio, 2008.

[56] C. Spiegel. *PEM Fuel cell modelling and simulation using MATLAB®.* Elsevier Inc., 2008.

[57] M.M. Mench. *Fuel Cell Engines.* John Wiley and Sons, Inc., 2008.

[58] L. Landis and J.L. Tucker. Making better fuel cells: Through-plane resistivity measurement of graphite-filled bipolar plates, 2002. Keithley Instruments Inc.: Cleveland, OH.

[59] B.D. Cunningham and D.G. Baird. Development of bipolar plates for fuel cells from graphite filled wet-lay material and a compatible thermoplastic laminate skin layer. *Journal of Power Sources*, 168(2):418–425, 2007.

[60] J.M. Hodgkinson. Mechanical testing of advanced fibre composites, 2000. CRC Press.

[61] V. Mishra, F. Yang, and R. Pitchumani. Measurement and prediction of electrical contact resistance between gas diffusion layers and bipolar plate for applications to pem fuel cells. *ASME Journal of Fuel Cell Science and Technology*, 1:2–9, 2004.

[62] L. Zhang, Y. Liu, H. Song, S. Wang, Y. Zhou, and S. J. Hu. Estimation of contact resistance in proton exchange membrane fuel cells based on experimental constitutive relation. *Journal of Power Sources*, 162(2):1165–1171, 2006.

[63] E.J. Carlson. Cost analysis of pem fuel cell systems for transportation, 2005. TIAX, LLC Cambridge, Massachusetts.

[64] S.K. Kamarudin. Technical design and economic evaluation of a pem fuel cell system. *Journal of Power Sources*, 157(2):641–649, 2006.

[65] I. Bar-On, R. Kirchain, and R. Roth. Technical cost analysis for pem fuel cells. *Journal of Power Sources*, 109(1):71–75, 2002.

[66] Bates Alex, Mukherjee Santanu, Sunwook, Sang Hwang, C. Lee, Kwon Osung, Choi Gyeung, and Park Sam. Simulation and experimental analysis of the clamping pressure distribution in a pem fuel cell stack. *International journal of hydrogen energy*, 38:6481–6493, 2013.

[67] W.R. Chang, J.J. Hwang, F.B. Weng, and S.H. Chan. Effect of clamping pressure on the performance of a pem fuel cell. *Journal of Power Sources*, 166:149–154, 2007.

[68] Lee Woo-kum, Ho Chien-Hsien, J.W. Van, and Murthy Mahesh. The effects of compression and gas diffusion layers on the performance of a pem fuel cell. *Journal of Power Sources*, 84:45–51, 1999.

[69] P. Zhou, C.W. Wu, and G.J. Ma. Influence of clamping force on the performance of pemfcs. *Journal of Power Sources*, 163:874–881, 2007.

[70] Lee Shuo-Jen, Hsu Chen-De, and Huang Ching-Han. Analyses of the fuel cell stack assembly pressure. *Journal of Power Sources*, 145:353–361, 2005.

[71] Na-Yu Ha, Su-Kim Seong, Do-Suh Jung, and Lee Dai-Gil. Composite endplates with pre-curvature for pemfc (polymer electrolyte membrane fuel cell). *Composite Structures*, 92:1498–1503, 2010.

[72] Liu Dongan, Peng Linfa, and Lai Xinmin. Effect of dimensional error of metallic bipolar plate on the gdl pressure distribution in the pem fuel cell. *International Journal of hydrogen energy*, 34:990–997, 2009.

[73] Lin Jui-Hsiang, Chen Wei-Hung, Su Yen-Ju, and Ko Tse-Hao. Effect of gas diffusion layer compression on the performance in a proton exchange membrane fuel cell. *Fuel cell*, 87:2420–2424, 2008.

[74] P. Zhou, C.W. Wu, and Z. Li. Effect of nonuniformity of the contact pressure distribution on the electrical contact resistance in proton exchange membrane fuel cells. *International Journal of hydrogen energy*, 36:6039–6044, 2011.

[75] Avasarala Bharat and Haldar Pradeep. Effect of surface roughness of composite bipolar plates on the contact resistance of a proton exchange membrane fuel cell. *Journal of Power Sources*, 188:225–229, 2009.

[76] Wen Chih-Yung, Lin Yu-Sheng, and Lu Chien-Heng. Experimental study of clamping effects on the performances of a single proton exchange membrane fuel cell and a 10-cell stack. *Journal of Power Sources*, 192:475–485, 2009.

[77] R. Montanini, G. Squadrito, and G. Giacoppo. Measurement of the clamping pressure distribution in polymer electrolyte fuel cells using piezoresistive sensor arrays and digital image correlation techniques. *Journal of Power Sources*, 196:8484–8493, 2010.

[78] Qing-Xing Xiu, Lum Kah-Wai, Joo-Poh Hee, and Ling-Wu Yan. Optimization of assembly clamping pressure on performance of proton-exchange membrane fuel cells. *Journal of Power Sources*, 195:62–68, 2010.

[79] Mehboob Hassan, Myung-Kyun Park, An-Soo Kang, Ahmed Behzad, and Ali Rashid. Analysis of the clamping pressure effect in pem fuel cell structure by fem and experiment, 2009.